

Hard Hill experimental plots on Moor House – Upper Teesdale National Nature Reserve

A review of the experimental set up

First published 28 July 2020

www.gov.uk/natural-england



Foreword

Natural England commission a range of reports from external contractors to provide evidence and advice to assist us in delivering our duties. The views in this report are those of the authors and do not necessarily represent those of Natural England.

Background

The Hard Hill experimental plots on Moor House NNR were established in 1954 to investigate the interaction between prescribed burning and grazing upon blanket bog vegetation in the North Pennines. The treatments (burning on short (10-year) and longer (20-year) rotations, no-burning, grazing and no-grazing) have been continued and since their initiation and the experiment has been the subject of numerous investigations.

In recent years, there has been discussion as to how comparable the blocks and plots are, and this project was initiated to investigate the similarities and differences between the blocks and plots to help guide new research in addition to revisiting previous findings.

This report should be cited as:

CLUTTERBUCK, B., LINDSAY, R, CHICO, G., CLOUGH, J. 2020. *Hard Hill experimental plots on Moor House – Upper Teesdale National Nature Reserve. A review of the experimental set up.* Natural England Commissioned Report No321

Natural England Project Manager - Alistair Crowle

Contractor - B Clutterbuck and R Lindsay

Keywords – Moor House, Hard Hill, blanket bog, morphology, micro-erosion, micro-topography, peat depth, nanotope features, burning, Sphagnum

Further information

This report can be downloaded from the Natural England Access to Evidence Catalogue: <http://publications.naturalengland.org.uk/> . For information on Natural England publications contact the Natural England Enquiry Service on 0300 060 3900 or e-mail enquiries@naturalengland.org.uk.

This report is published by Natural England under the Open Government Licence - OGLv3.0 for public sector information. You are encouraged to use, and reuse, information subject to certain conditions. For details of the licence visit [Copyright](#). Natural England photographs are only available for non-commercial purposes. If any other information such as maps or data cannot be used commercially this will be made clear within the report.

ISBN 978-1-78354-649-7

© Natural England and other parties 2020



Hard Hill experimental plots on Moor House – Upper Teesdale National Nature Reserve

A review of the experimental setup

**Hard Hill experimental plots
on Moor House – Upper Teesdale
National Nature Reserve**

A review of the experimental setup

Submission to Natural England – June 2020

**Ben Clutterbuck
Richard Lindsay
Guaduneth Chico
Jack Clough**

Acknowledgements

This project was funded by Natural England with equipment and staff time supported by Nottingham Trent University and University of East London through the UKRI QR Strategic Priorities Fund.

The project has been overseen by Alistair Crowle at Natural England and we are grateful for his input, guidance and flexibility. Additional comments on an earlier draft were made by Dave Glaves and Alice Noble at Natural England.

We would like to thank Martin Furness at Natural England, and Chris and Heather McCarthy (formerly Natural England), for their help in facilitating access to Moor House-Upper Teesdale NNR. We also thank Dave Glaves for providing copies of early Nature Conservancy reports and Rob Rose of CEH for providing scanned NERC aerial photographs for 1995.

Author contact details:

Dr Ben Clutterbuck

School of Animal, Rural and Environmental Sciences
Nottingham Trent University
Brackenhurst
Southwell
NG25 0QF

T: +44 (0)115 848 5320
M: +44 (0)7890 316813

Email: ben.clutterbuck@ntu.ac.uk

Richard Lindsay

Sustainability Research Institute
Knowledge Dock
Docklands Campus
University Way
London
E16 2RD

T: +44 (0)20 8223 4088
M: +44 (0)7739 479122

Email: r.lindsay@uel.ac.uk

Summary

The Hard Hill Experiment is assumed to consist of replicated treatments involving fire-rotation lengths and grazing. In reality, the various treatment plots are not replicates of comparable treatments because significant differences have been identified between the various plots in terms of their physical structure and treatment history.

The Hard Hill experimental blocks already had a varied history of burning when they were established, with some plots displaying clear evidence of recent burn scars prior to the 1954 burn undertaken at the start of the experiment. These scars remained evident for a considerable number of years after this 1954 burn and indeed after subsequent burns.

The pattern of experimental burning since the start of the experiment has not always followed the precise boundaries of the treatment plots, resulting in fire effects even within parts of treatment plots that are designated as 'no-burn after 1954'.

Almost half of the plots burned in 1954 and not burned since contain significant meso-scale structural features that demonstrably affect the vegetation and microtopography within their vicinity – probably more so than the experimental treatments applied to each plot.

Peat 'softness', as measured by a specially-designed penetrometer for use in peat, appears to be the most effective measure of bog condition and time-since-fire, particularly when combined with the nature of the microtopography and associated vegetation types. In general, the more distant the last fire event the softer the peat surface, though tussocks should not be included in such testing because these features tend to be very dense and do not necessarily reflect the condition of the surrounding peat.

Frequent burning has tended to create a surface micro-relief in which micro-erosion and tussocks are the dominant features of the microtopography. This provides an interconnected drainage network that facilitates comparatively rapid loss of surface water compared with areas possessing more *Sphagnum* cover, particularly as peat is shown to be denser and thus more resistant to infiltration of surface water across areas that are regularly burnt.

Frequent burning can create a waterproof layer at the peat surface within which pockets of *Sphagnum* may escape fire damage or can subsequently become established, but these pockets seem to have remained restricted in their ability to expand and generate a more continuous and naturally functioning *Sphagnum* sward. Repeated burning appears to have held the vegetation and microtopography in a form of 'arrested development'. Overall, the trend in such areas has been a diminution of *Sphagnum* cover, or, at best, maintenance as individual constrained patches.

Cessation of burning on an already burnt site has nevertheless resulted in loss of the limited existing *Sphagnum* presence as growth of tussock-forming species, together with *Calluna vulgaris*, have proceeded to dominate the bog surface. Over a period of several decades, however, mosses such as *Hypnum jutlandicum* have formed continuous swards beneath the *Calluna* canopy, slowing water movement from the site and thereby increasing surface wetness, ultimately providing opportunities for *Sphagnum* to re-establish. In addition, the humid shelter provided particularly by the tussock and/or *Calluna* canopy have also enabled *Sphagnum* to re-establish. Timescales for this process appear to exceed a century – but such timescales of recovery are readily understood when applied to woodland restoration and, given that peat bog systems are generally as old as, if not older than, most woodland stands, it is important to recognise the need to apply similar recovery timescales when considering

the management and restoration of peat bog systems following emergence from a long history of burning management and other pressures such as atmospheric pollution.

In order to provide a long-term visual record for the Hard Hill Experiment, a permanent 2019 photo-archive baseline for each treatment plot in each block has been created – the first of its kind for the site. This photo archive is now held in the University of East London open-access Data Repository. These images consist of 360° 2D and 180° 3D imagery which can be viewed using smartphones or computers, and can be viewed immersively using simple VR goggles with smartphones or using full VR headsets. Permanent monitoring markers of a type recommended within the IUCN UK Peatland Programme 'Eyes on the Bog' Programme have also been installed in all plots within Block D, and the boundary of the grazed portion of Block D has been similarly marked.

Contents

Acknowledgements	ii
Summary.....	iii
Contents.....	v
List of tables	vii
List of figures	viii
1 Introduction.....	1
1.1 Establishment of the Hard Hill Experimental Plots	1
1.2 Aims and objectives of the present study	4
2 Historical reconstruction of Hard Hill and the surrounding NNR	5
2.1 Image sources	5
2.2 Aerial imagery - 1953.....	6
2.3 Aerial imagery – 1960 and 1966	7
2.4 Aerial imagery – 1966	8
2.5 Aerial imagery – 1969	9
2.5.1 Erosion features.....	10
2.5.2 Visible persistence of pre-experimental burn scars	13
2.6 Aerial imagery – 1992	16
2.7 Aerial imagery – 1995	17
2.7.1 Inconsistent burn extents	17
2.8 Aerial imagery – 2002-2018	19
3 Gross morphology and micro-relief of the experimental blocks and plots	22
3.1 Slope	22
3.1.1 Slope across experimental blocks.....	22
3.1.2 Slope across plots	24
3.2 Effect of micro-relief on slope values	25
3.3 Drainage patterns	27
3.4 Peat depth	29
4 Micro-relief components (nanotopes) and vegetation	31
4.1 Context	31
4.2 Methods.....	32
4.2.1 VR imagery	32
4.2.2 Peat density – use of penetrometer	33
4.2.3 Bog microtopography and vegetation.....	34

4.3	Results.....	35
4.3.1	VR imagery.....	35
4.3.2	Penetrometer results – bulk density and bog ‘softness’.....	36
4.3.3	Vegetation in Block D and additional plots.....	39
4.3.4	Nanotopes in Block D and additional plots.....	43
5	‘Eyes on the Bog’ long term markers.....	48
6	Synthesis.....	49
6.1	Meso-scale features within the treatment plots.....	49
6.2	Fire treatments within the individual plots.....	49
6.3	Ecological condition of Block D and supplementary plots.....	50
7	Recommendations.....	53
8	References.....	54
	Appendix 1.....	57
	Re-working of data from Lee et al. (2013).....	57

List of tables

Table 1 Conventional aerial photography and UAV-derived imagery used in this research...	5
Table 2 Dates of burning undertaken across experimental plots on Hard Hill.	8
Table 3 Slope of terrain in experimental blocks on Hard Hill derived from airborne Lidar (DTM).	23
Table 4 Mean (\pm SD) slope determined for individual plots on Hard Hill derived from TLS DTM (green and red indicate lowest and highest mean values of slope respectively by fenced (F) and grazed (G) areas).....	27
Table 5 Peat depth across experimental blocks on Hard Hill.	30
Table 6 Categories used for nanotope and vegetation mapping – see also Section 24 of Lindsay (2010) for further details of nanotope types.....	35
Table 7 Presence-absence species data assembled by Lee et al. (2013) presented using phytosociological sorting.	57

List of figures

Figure 1 Location of Moor House–Upper Teesdale NNR and Hard Hill experimental blocks.	2
Figure 2 Location of experimental blocks and arrangement of treatments in relation to topography on Hard Hill. RGB imagery captured by senseFly eBee in September 2017.	3
Figure 3 Hard Hill in 1953 showing location of grouse butts and recent burn scars.	6
Figure 4 Hard Hill in 1953 showing location of grouse butts and recent burn scars in relation to the location of the experimental blocks.....	7
Figure 5 Hard Hill in 1960 showing location of the burn scars undertaken at the start of the experiment.	8
Figure 6 Hard Hill in 1966 showing location of burns undertaken in 1965 inside 10-year plots and burns from other years outside the experimental area.....	9
Figure 7 Hard Hill in 1969 showing that no further burning had occurred in the NNR since 1966.....	10
Figure 8 Presence of meso-scale erosion gullies in experimental Block D. The imagery for 2015 shows a model of the peat surface underneath vegetation extracted from TLS survey.	11
Figure 9 Presence of erosion feature in experimental block A.	12
Figure 10 Impact of pre-experimental burn on vegetation in experimental block B.	13
Figure 11 Impact of pre-experimental burn on experimental block A.	15
Figure 12 Hard Hill in 1992 showing location of burns undertaken in 1985/6 (inside 10-year plots and outside).....	16
Figure 13 Hard Hill in 1995 showing location of burns undertaken in 1994/5 (inside 10- and 20-year plots).....	17
Figure 14 Inconsistent burn extents in experimental block D.	18
Figure 15 Hard Hill in 2002 showing location of burns undertaken in 1994/5 (inside 10- and 20-year plots).....	19
Figure 16 Hard Hill in 2010 showing location of burns undertaken in 2007 (inside 10-year plots).....	20
Figure 17 Hard Hill in 2015 showing location of burns undertaken in 2007 (inside 10-year plots).....	20
Figure 18 Hard Hill in 2018 showing location of burns undertaken in 2017 (inside 10- and 20-year plots).....	21
Figure 19 Topography of Hard Hill visible in airborne Lidar (DTM) and UAV derived DSM (hillshade view shown).	23
Figure 20 Slope of the terrain across experimental blocks on Hard Hill derived from airborne Lidar (DTM).....	24

Figure 21 Slope of the terrain across plots (grouped by burn treatment per block) on Hard Hill derived from airborne Lidar (DTM).	24
Figure 22 DTM derived from TLS survey for block D showing area assessed for plot level slope analysis (note the visible depressions in the peat surface created by persistent footfall since 1954, particularly around edges of plots and along the fence lines).	26
Figure 23 Surface water flow modelled for Hard Hill from airborne lidar DTM and UAV derived DSM data.	28
Figure 24 Surface water flow modelled for experimental blocks on Hard Hill from TLS derived DTM data (each block oriented approximately uphill).	29
Figure 25 Peat depth across experimental blocks on Hard Hill (location of two additional plots surveyed in 2019 shown).	30
Figure 26 Example of a 360° 2D view of the 1954-burn fenced treatment plot in Block D... ..	33
Figure 27 Penetrometer for use on peat soils. (left) Components of the penetrometer. (right) Penetrometer in use in the field.....	34
Figure 28 Individual values for cavity strength obtained from each sample point along each transect within Block D and in the new plots adjacent to Block D. Data points have been grouped into plot treatments. '10 yr f' = burnt every 10 years, fenced; '20 yr f' = burnt every 20 years, fenced; '1954 f' = burnt only in 1954, fenced; '10 yr g' = burnt every 10 years, grazed; '20 yr g' = burnt every 20 years, grazed; '1954 g' = burnt only in 1954, grazed; '1954 only' = new plot, burnt during the 1954 fire but located outside Block D, grazed; 'Pre-1954' = new plot, last burnt at some date prior to 1954 (potentially >95 years ago), grazed.	36
Figure 29 Map of cavity strength (i.e. peat 'hardness') for Block D and new supplementary plots, with sample points affected by meso-scale features removed (small black dots), and with the most dense tussocks indicated by pale yellow dots rather than cavity-strength values.	37
Figure 30 The data for cavity strength presented in Figure 28 now displayed as box plots, with the upper range of values truncated at 9,000 N m ⁻² to remove the dense outliers largely representing tussocks. Data are grouped according to plot treatments. '10 yr f' = burnt every 10 years, fenced; '20 yr f' = burnt every 20 years, fenced; '1954 f' = burnt only in 1954, fenced; '10 yr g' = burnt every 10 years, grazed; '20 yr g' = burnt every 20 years, grazed; '1954 g' = burnt only in 1954, grazed; '1954 only' = new plot, burnt during the 1954 fire but located outside Block D, grazed; 'Pre-1954' = new plot, last burnt at some date prior to 1954 (potentially >95 years ago), grazed.	38
Figure 31 Total cumulative Domin scores for all <i>Sphagnum</i> species recorded in Block D in 1961 to show relative cover of <i>Sphagnum</i> in the six treatment plots of Block D.	40
Figure 32 Distribution of <i>Sphagnum</i> cover in Block D for 1961 and 2019. Values for 1961 are Domin scores (sized red circles) while 2019 are presence/absence data (black circles).	

Small black dots indicate all sampling locations for 2019. The TLS ground survey data are displayed as background to the main Block D. 41

Figure 33 Cumulative occurrences of *Sphagnum* species within each treatment plot in Block D recorded in 2019. 41

Figure 34 Rejuvenated *Calluna* stems layering in a *Sphagnum capillifolium* hummock within the grazed, burnt-1954 only, Block D, treatment plot..... 42

Figure 35 Percentage occurrence for micro-erosion and tussock nanotopes across the various plot treatments in Block D, based on sample points not affected by meso-scale features..... 44

Figure 36 Distribution pattern of micro-erosion, tussocks, *Sphagnum* and hypnoid mosses across all plots associated with Block D. Different elements are displayed with the largest symbol to the rear and the smallest to the fore so that all co-occurrences can be seen. The meso-scale landscape features identified by TLS mapping within Block D are displayed as background for the six original treatment plots. 45

Figure 37 Differing examples of natural blanket bog systems. (left) *Sphagnum*/low dwarf shrub community; (centre) *Sphagnum*/cotton grass community; (right) *Sphagnum*/short sedge community. (left) Inverness-shire; (centre) Border Mires; (right) Sutherland. 46

Figure 38 Differing examples of degraded blanket bog systems dominated by tussock and micro-erosion from 10-year or 20-year treatment plots at Hard Hill. (left) *Calluna*/*Trichophorum*-bare peat; (centre) Cotton grass-bare peat; (right) Cotton grass/short mosses-bare peat. 46

Figure 39 A natural *Sphagnum*-rich bog surface has undulations that characteristically lie across the line of water movement. These undulations slow down seepage across the bog surface even if the peat is fully saturated. 47

Figure 40 A bog surface reduced to tussocks of cotton grass (*Eriophorum vaginatum*), deer-hair grass (*Trichophorum cespitosum*), purple-moor grass (*Molinia caerulea*) or wavy hair grass (*Deschampsia flexuosa*) with essentially bare peat between the tussocks has less capacity to slow down surface-water movement, even if there are occasional patches of *Sphagnum* or other mosses. 47

Figure 41 The visible blue top plate of a permanent metal marker indicates the SW corner of the grazed sector of Block D. Similar markers indicate the NW corner of the grazed sector as well as the fixed-photography points in the centres of each treatment plot. 48

Figure 42. Lesser twayblade (*Neottia [Listera] cordata*), a delicate ‘sphagnophile’ now recorded from the Reference plots but not yet recorded within the experimental plots. 52

Figure 42. Lesser twayblade (*Neottia [Listera] cordata*), a delicate ‘sphagnophile’ now recorded from the Reference plots but not yet recorded within the experimental plots.

1 Introduction

1.1 Establishment of the Hard Hill Experimental Plots

Moor House–Upper Teesdale National Nature Reserve (NNR) is located in the North Pennines Area of Outstanding Natural Beauty (AONB) and divided into two sections on the northwest and southeast sides of Cow Green Reservoir (Figure 1). The Hard Hill experiment, located in the northwest section of the NNR, was initiated by the Nature Conservancy (NC) in 1954. The objective was to establish a series of randomised replicated plots to monitor the effects of grazing and rotational burning treatments on blanket bog vegetation and soil fertility (Elliott, 1958). Four blocks (A-D) were established, each comprising six treatment plots measuring approximately 30m x 30m (Figure 2). All blocks were entirely burnt at the start of the experiment to the extent that “...*all vegetation was eliminated...*” (Forrest, 1961). Half of each block was then fenced to exclude grazing, and three rotational burning treatments were subsequently replicated in both halves. The various plots were originally labelled according to the block letter and the treatments applied (Forrest, 1961), thus using Block A as an example:

- A/S – short-rotation cycle of approximately 10 years between burns, grazed;
- A/SF – short-rotation cycle of approximately 10 years between burns, fenced;
- A/L – long-rotation cycle of approximately 20 years between burns, grazed;
- A/LF – long-rotation cycle of approximately 20 years between burns, fenced;
- A/N – burned in 1954 only, grazed;
- A/NF – burned in 1954 only, fenced.

In addition, a reference plot outside each block was left unburned in 1954 and has not been burned since. These plots have been labelled as ‘R’ plots in subsequent literature. The precise location of these four reference plots is, however, now uncertain.

The original labelling of ‘N’ for the plots burned only in 1954 is unfortunate because ‘N’ has since given rise to widespread use of the terms ‘no-burn’ or ‘unburnt’ plots when in fact they, along with the short- and long-rotation burn plots were burnt, apparently quite severely, in 1954 and thus demonstrate long-term recovery from fire rather than representing the natural unburnt state. This is an important consideration when interpreting results from these plots, and so to be clear about the processes under consideration, in the present report the burning treatments are referred to as:

- ‘10, or 10-year’ – for the short 10-year burning cycle;
- ‘20, or 20-year’ – for the longer 20-year burning cycle; and
- ‘54, or burnt 1954’ - for the plots burnt in 1954 only.

Using this approach to treatment labelling, Figure 2 displays the layout of the Hard Hill Plots in relation to the macro- and meso-scale features of the Hard Hill area. The footprints of the experimental blocks and component plots shown in all Figures within the present report were digitised from UAV imagery captured in 2017.

Although the design of the experiment appears to provide a series of replicated plots for comparison, the micro-relief (microtopography) of the plots and meso-scale morphology of the plots and immediate surrounding areas have not been reported nor been included in studies assessing differences between treatments. Furthermore, the vegetation of the plots was not recorded prior to the initial fire of 1954, giving rise to uncertainty about the baseline condition of the ground prior to the first experimental burn. Moreover, when Forrest (1961) describes the initial fire in 1954 as having eliminated all vegetation, it is not clear whether this means *all*

vegetation including the entire bryophyte layer, or whether this refers largely to elimination of the vascular plant layer.

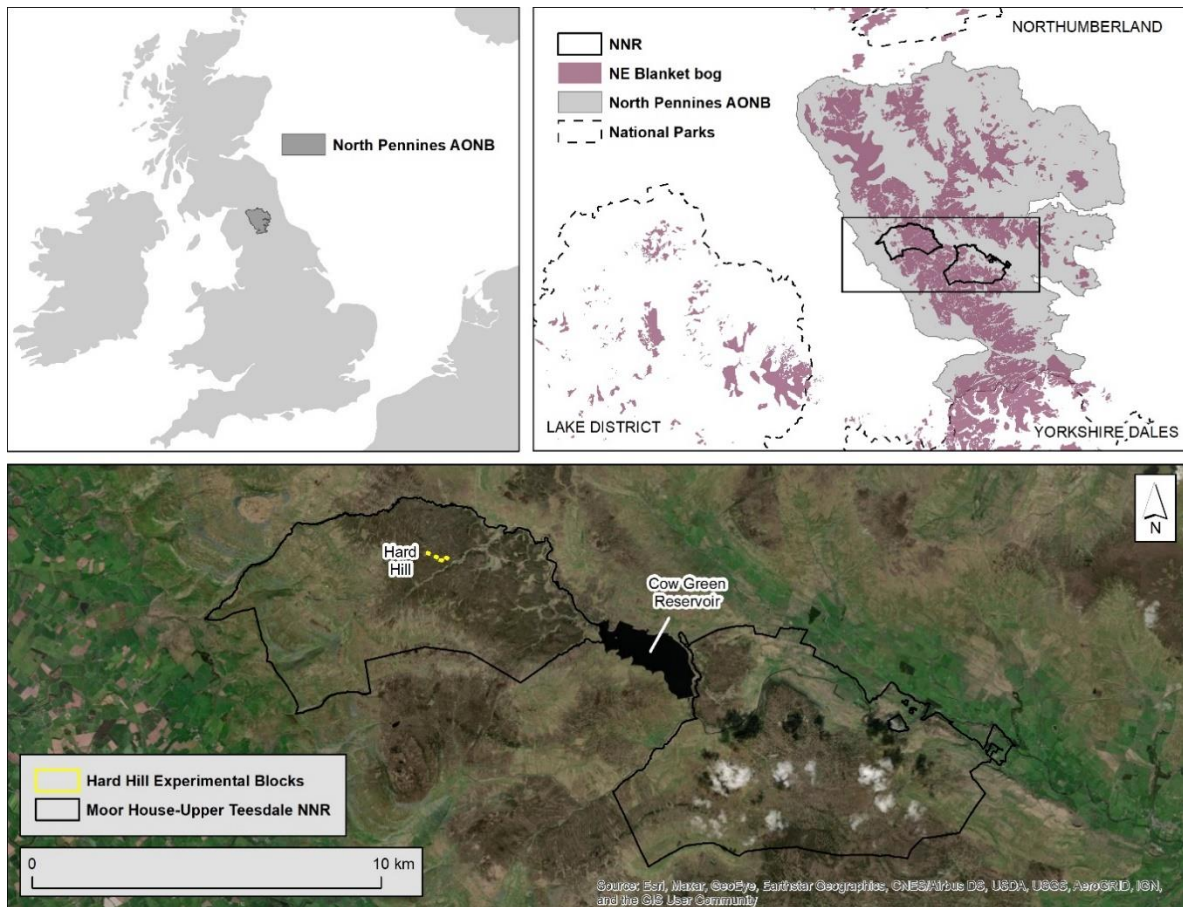


Figure 1 Location of Moor House–Upper Teesdale NNR and Hard Hill experimental blocks.

There was in fact no vegetation monitoring until seven years after the initial fire, at which point Forrest (1961) surveyed the vegetation of the experimental plots as well as “*adjacent representative areas of unburnt moorland*” – specifically using 10 quadrats adjacent to each of Blocks B and C and five adjacent to Block A on the assumption that these would reflect the original state of the vegetation within the experimental plots prior to the 1954 burn and thus act as experimental controls. Notwithstanding Forrest’s assumption about the representative nature of the quadrats taken adjacent to the experimental blocks, the actual post-fire condition of the blocks remains uncertain because no recording was undertaken either immediately prior to or subsequent to the 1954 fire event. There are thus no true baseline data for this experiment in terms of vegetation, micro-relief or meso-scale physical features. Such information is essential not only in terms of making a sound determination concerning the original comparability of the replicate blocks and treatment plots but also as the foundation for all subsequent analysis of change.

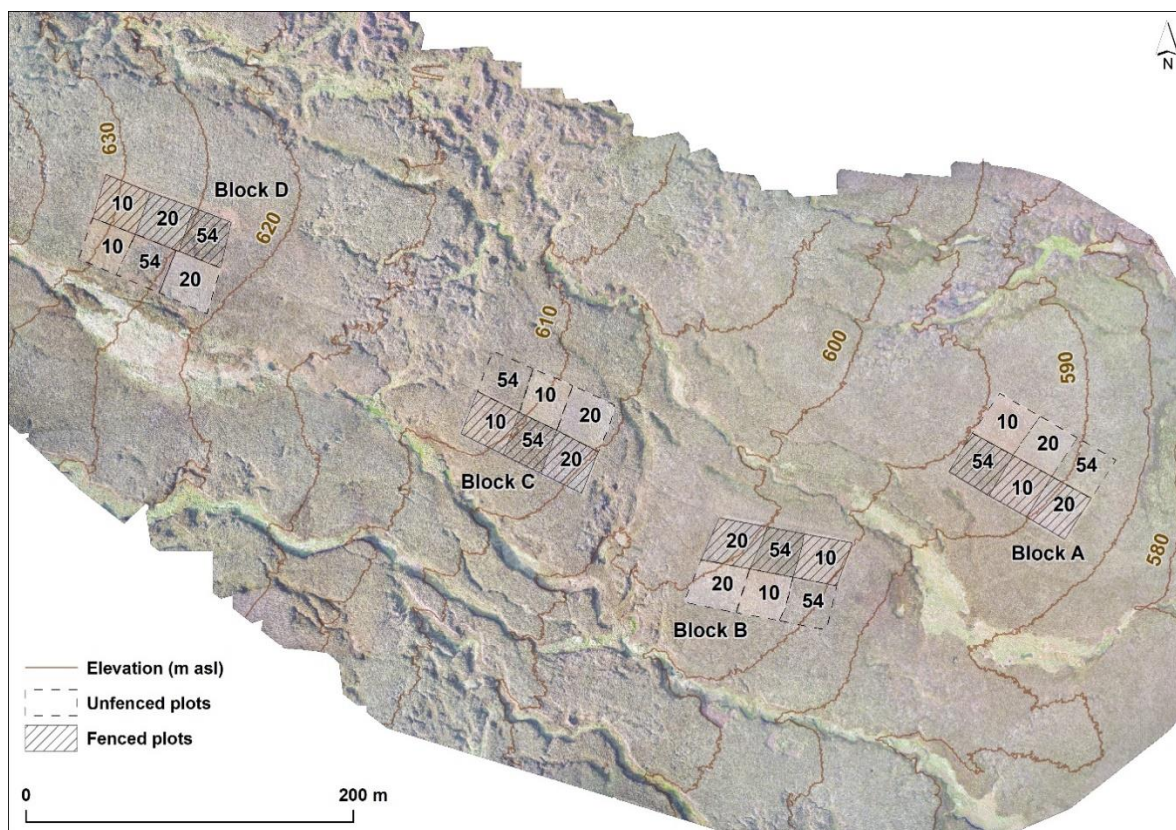


Figure 2 Location of experimental blocks and arrangement of treatments in relation to topography on Hard Hill. RGB imagery captured by senseFly eBee in September 2017.

It is also important to note that Forrest (1961) describes the Hard Hill area as “a large area of degenerated blanket bog” and that the study sought to “compare the vegetation which results after seven years’ regeneration with the vegetation of adjacent moorland which had not been burnt for many years, hereinafter referred to as unburnt moorland”. The study was thus set within an area of blanket bog acknowledged as being degraded rather than bog in a natural or near-natural state, and although the area is described as having been burnt “many years” ago, no timescale is provided for the duration of this fire-free period though Rawes and Hobbs (1979) state that in 1954 the reference plots had been “unburnt for >30 years”. Furthermore, the main objective of the study was to investigate the effects of burning and grazing treatments on the vascular plant cover. Rawes and Hobbs (1979) report results for vascular plants such as *Eriophorum vaginatum* and *Calluna vulgaris* but have little to say about *Sphagnum* or other elements of the moss layer, other than to note that *Sphagnum capillifolium* was one of the community dominants. It is therefore entirely possible that when the initial experimental fire was described as having eliminated all vegetation this referred only to the vascular plant cover and did not mean that the surface moss layer was also entirely removed. Indeed, data from 1961, referred to later in the present report, strongly suggests that the initial fire did not reduce the whole experimental surface to burnt bare peat.

Forrest’s (1961) account thus establishes valuable contextual information about the original Hard Hill study, namely that the blocks are set within an area of degraded blanket bog having a history of burning and grazing. Any control or reference data from ground outside the areas burnt in 1954 can thus be expected to reflect this degraded condition-state, as well as potentially displaying a trajectory of recovery from past impacts, albeit further along this trajectory of recovery (potentially 30-40 years further) than anything observed within the experimental blocks.

1.2 Aims and objectives of the present study

The present study aims to begin addressing some of the information-gaps currently hampering better understanding of the experimental results obtained from the Hard Hill experiment. It does so by providing, for the first time, an assessment of the likely broad condition-state of vegetation, at least in terms of past fire impacts and large-scale erosion patterns, within and around the experimental blocks prior to the start of the experiment and then through the course of the experiment. It also provides the first detailed description of landform morphology for the whole Hard Hill experimental area as well as identifying meso-scale landform features within the blocks themselves. Finally, it explores the potential information-value, in terms of condition-state and recovery process, offered by micro-landscape (microtopography) features observable within the experimental plots – specifically the small-scale structures or nanotopes (Lindsay, 2010; Joosten et al., 2017) that are such a characteristic and distinctive feature of peat bog ecosystems.

Various objectives were thus defined at a range of scales.

For all experimental blocks:

- use historical aerial photography to understand vegetation conditions across the site prior to the start of the experiment;
- provide definitive descriptions of the gross morphology of the plots and surrounding areas;
- assess microtopographic variation across the plots;
- map peat depth across all plots;
- set up long-term monitoring of the plots aligned with the IUCN UK Peatland Programme 'Eyes on the Bog' monitoring protocol (Lindsay et al., 2019) to include, for each plot:
 - ground-level subsidence due to shrinkage;
 - general water-table conditions;
 - 360° VR and stereo VR photographs from the centre of each plot.

For all plots in Block D, plus for two additional plots newly establishing during the present study and located outside, but close to, Block D:

- define nanotope features and background micro-landscape network;
- record synusial vegetation of nanotope features.

2 Historical reconstruction of Hard Hill and the surrounding NNR

2.1 Image sources

Historical aerial photographs covering Hard Hill were obtained for 1953 (one year prior to initiation of the experiment) and for nine subsequent time periods up to 2018 (Table 1). Aerial imagery post-2002 were delivered as orthorectified products. Imagery for the years 1953, 1966, 1969, 1992 and 1995 were provided as digital scans and were orthorectified in ERDAS Imagine 2020. Orthorectified imagery for the year 2018 and an Ordnance Survey digital terrain model (OS DTM) at 5 m resolution were used to obtain x, y and z coordinates in the British National Grid to provide control points for image correction. The root mean square error (RMSE) of orthorectification for each image was less than one pixel thereby providing very strong alignment of imagery thereby providing considerable confidence when mapping the evolution of features on Hard Hill through time (Table 1). An additional low-resolution image of an aerial photograph from 1960 was provided by Natural England and this was georeferenced in ArcGIS.

Hard Hill was also flown in 2017 and 2018 with a fixed-wing unmanned aerial vehicle (UAV) to collect ultra-high-resolution colour (RGB) imagery (Table 1). Twenty ground control targets were placed across Hard Hill to provide control points for orthorectification. The location of the targets was recorded using a Trimble R2 GNSS and the data post-processed using RINEX (Receiver Independent Exchange Format) data from the nearest OS Net base station located at Wearhead (13 km north-east). Positional data corrected to within 1.5 – 1.7 cm (x and y) and 2.1 – 2.4 cm (z), and the RMSE of orthorectification for each set of imagery was less than one pixel (Table 1). Digital surface models (DSMs) of elevation were extracted from the RGB imagery. All UAV image processing was undertaken using Pix4Dmapper v4.3.33.

Table 1 Conventional aerial photography and UAV-derived imagery used in this research.

Year	Image date	Source	Format	Resolution	RMSE (pixels)
<i>Aerial photography</i>					
1953	30 June	Historic England	B&W	36 cm	0.19
1960	unknown	Natural England	B&W	1 m	-
1966	22 July	Historic England	B&W	45 cm	0.11
1969	10 October	Historic England	B&W	39 cm	0.07
1992	13 November	Old Aerial Photos	Colour (RGB)	50 cm	0.13
1995	06 August	NERC/CEH	Colour (RGB)	20 cm	0.18
2002	unknown	Infoterra (PGA)	Colour (RGB)	25 cm	-
2010	unknown	Edina Digimap	Colour (RGB)	25 cm	-
2015	unknown	Edina Digimap	Colour (RGB)	25 cm	-
2018	unknown	Edina Digimap	Colour (RGB)	25 cm	-
<i>UAV surveys</i>					
2017	28 September	Ben Clutterbuck	Colour (RGB)	1.8 cm	0.48
2018	26 June	Ben Clutterbuck	Colour (RGB)	1.6 cm	0.31

2.2 Aerial imagery - 1953

There is a long history of Moor House being managed as a grouse moor prior to the Nature Conservancy purchasing and designating the NNR in 1952. The earliest written record of shooting in the NNR dates to 1842 (Bell, 1843 cited in Taylor & Rawes, 1974), and the imagery from 1953 shows two lines of grouse butts on the northern and eastern flanks of Hard Hill (Figure 3). The southernmost line of butts is adjacent to the area of Hard Hill that was selected for the burning experiments in 1954. In the years immediately preceding this image, management of vegetation on Hard Hill predominantly comprised the burning of small patches (Figure 3). Some of these burns are adjacent to the grouse butts, and one recent burn (at the time of image capture) is in an area of vegetation that one year later (1954) becomes experimental Block B (Figure 4; Section 2.5.2). The age of this burn is estimated to be between 12-15 years (see sections 2.4-2.5). An older burn scar is also visible in an area of vegetation that became Block A. This burn may be between 15-30 years old, though more precise dating of this burn is less certain.

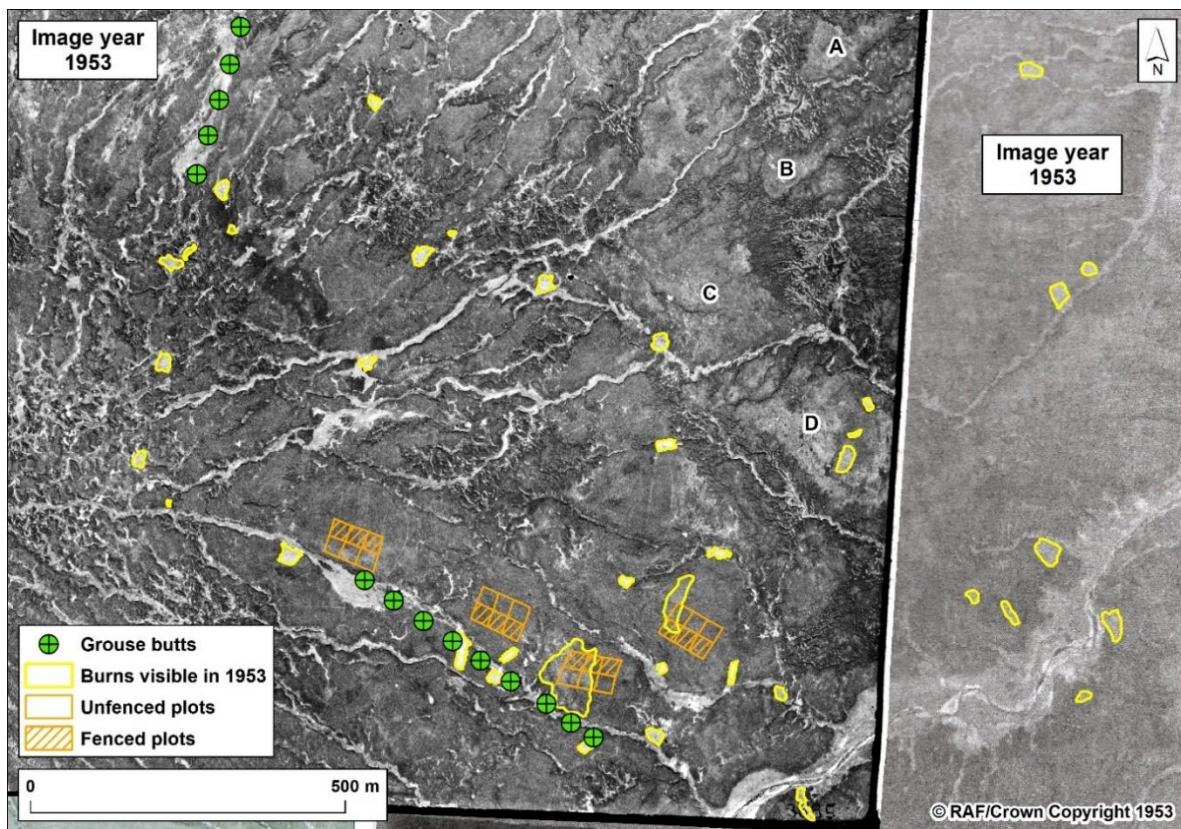


Figure 3 Hard Hill in 1953 showing location of grouse butts and recent burn scars.

Earlier approaches to vegetation management across Moor House reportedly burned far larger areas for both grouse and sheep farming. In the early 1900s, 250-500 acres (1-2 km²) were typically burned each year (Taylor & Rawes, 1974). It is not certain how or when burn sizes changed over time, but large burn scars up to 200 m wide are visible in 1953 at several locations (see e.g. A-D on Figure 3). It is evident, therefore, that at the start of the experiment, the vegetation across the area where the experimental blocks were created was of varying 'post-fire' age. It is also likely that the vegetation had experienced a range of repeat burn intervals since the 1800s. Although vegetation was not surveyed prior to the first burn in 1954, it is interesting to note that distinct differences in vegetation composition – specifically in

Calluna vulgaris, *Rubus chamaemorus*, *Eriophorum angustifolium* and *Sphagnum* spp. – were recorded between the experimental blocks in 1961 only 7 years after the experiment started (Hobbs, 1984).

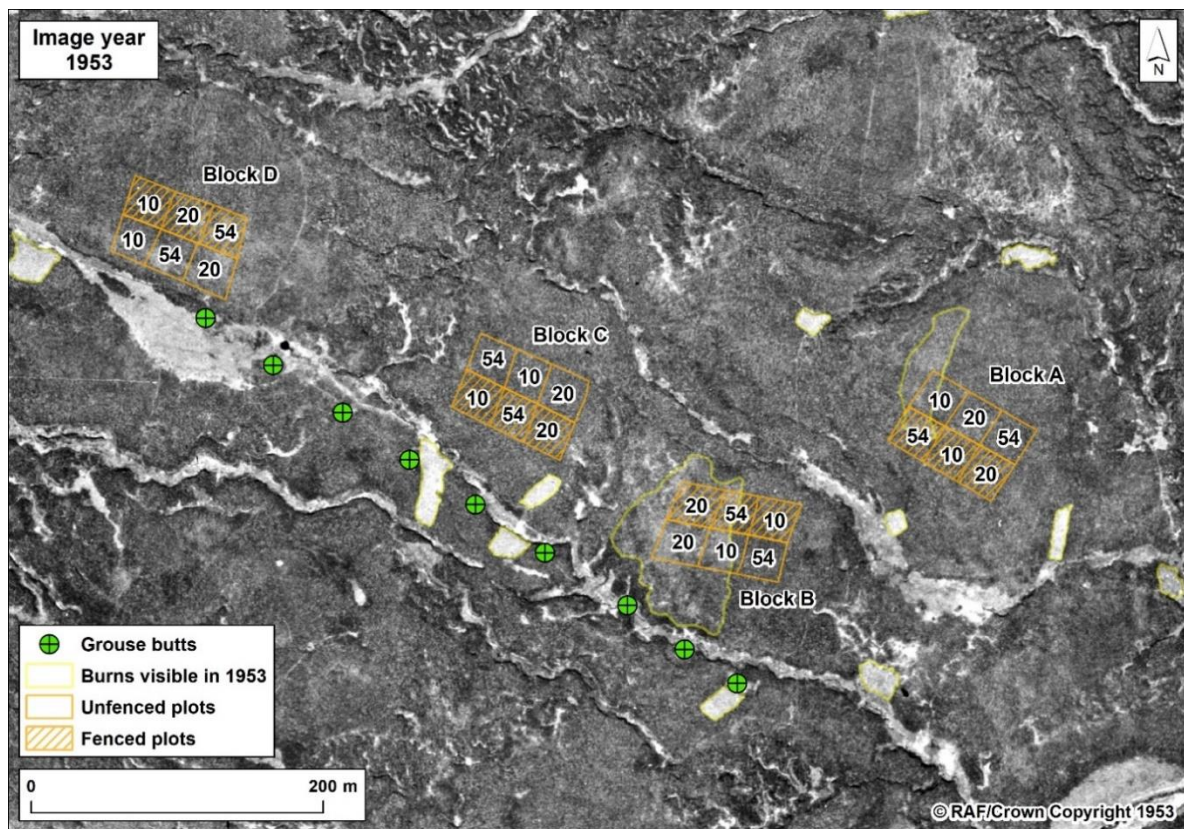


Figure 4 Hard Hill in 1953 showing location of grouse butts and recent burn scars in relation to the location of the experimental blocks.

2.3 Aerial imagery – 1960 and 1966

The aerial image from 1960 shows six large burn patches on Hard Hill (Figure 5). The extents of these were digitised with input from the high-resolution image from 1966 (Figure 6) to provide accurate geolocation of these burns. Five of these patches were burned on April 20th 1954, and the most south-easterly patch was reportedly burned in 1953 (Rawes, 1964; Taylor & Rawes, 1974).

Four of the patches burned in 1954 were selected as Blocks A-D for the experiment and fencing was installed by the Forestry Commission in 1957 (Rawes, 1965). The plots were only defined on the ground in 1961 (Forrest, 1961), and the 10- and 20-year plots identified were subsequently burned at intervals of approximately 10 and 20 years through to current day (Table 2).

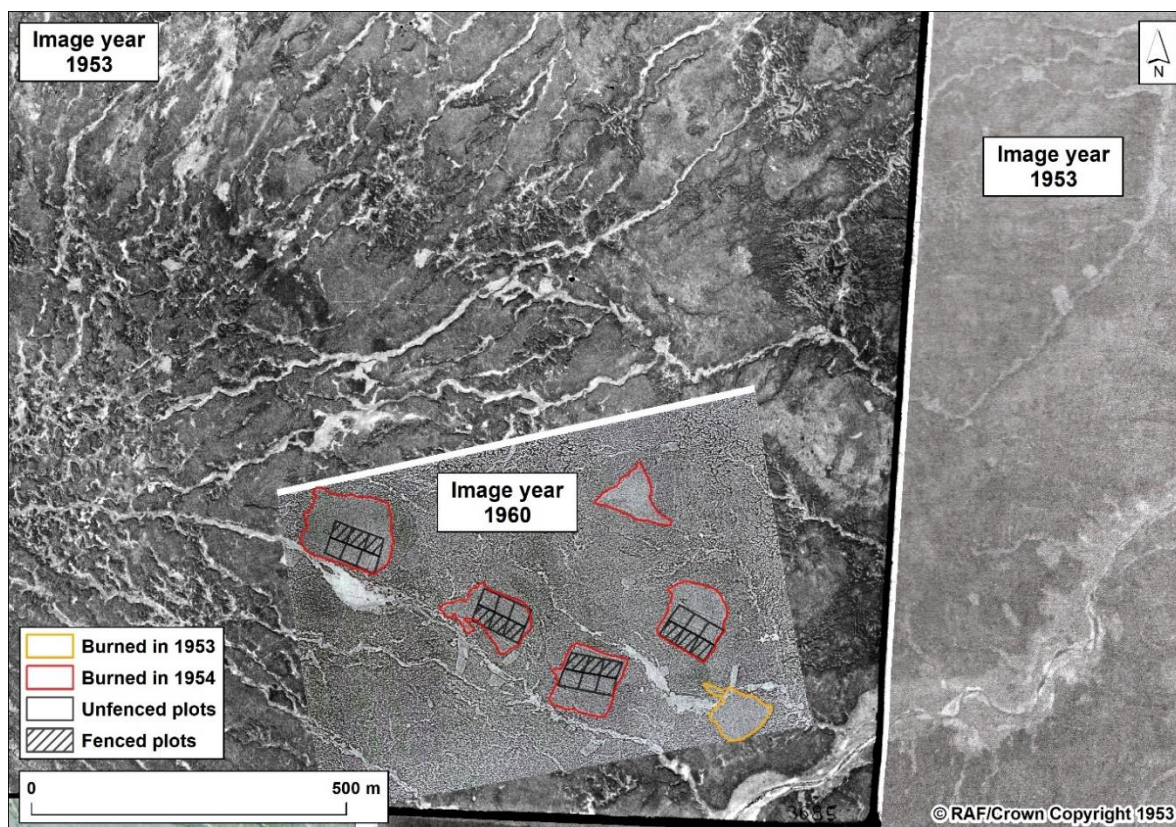


Figure 5 Hard Hill in 1960 showing location of the burn scars undertaken at the start of the experiment.

Table 2 Dates of burning undertaken across experimental plots on Hard Hill.

Plot	1954	1965	1975	1985/6	1994/5	2007	2017
burnt 54	X						
10-year	X	X	X	X	X	X	X
20-year	X		X		X		X

2.4 Aerial imagery – 1966

The 10-year plots in all four blocks were burned in March 1965, although burning had been attempted but aborted in the unfenced plot in Block A in 1964 (Rawes, 1965). The burn scars were digitised from the 1966 image, and it is clear for Blocks A-C that fire was not constrained solely to the experimental blocks (Figure 6) as some fire spread 30-70 m to the north-west (presumably in the direction of the wind). In addition, the burning of the plots in Blocks A and D is not consistent with the footprint of the plots burned in more recent years. In Block A the fire from the 10-year plots spread across part of the unfenced 20-year plot (see also Figure 9), burning 10-15% of the plot (Rawes, 1965). In Block D, fire from the 10-year grazed plot spread into part of the grazed plot not burned since 1954, and the 10-year fenced plot was not burned in its entirety (see also Figure 14). This observation highlights a clear change in the style and control of burning during the experiment (expanded section 2.7.1), something that was noted by Rawes (1965):

“Burns were on 30 March (M.R.) and 31 March (M.R., D.S., B.M.) and they were reasonably good except for A/S which had received abortive attempts at firing in 1964. Burning of small plots is extremely hazardous in dry conditions with strong wind, and several fires “got-away”. They were: from W. corner of C/SF, from N. corner of B/SF, N.W. from A/S and also from A/SF. The latter fire spread across the W. side of plot A/L and burnt 10-15% of it. In view of the impossibility of confining the fire in such small plots it is proposed to burn fire breaks around each block from time to time.”

Five large burn scars were also visible outside of the experimental blocks (Figure 6) and are reported to have occurred in 1956 (Rawes, 1965) and 1961 (Rawes, 1965; Taylor & Rawes, 1974). It is important to note that the outline of two of the burn patches from 1954 are barely discernible from the background vegetation in 1966 (12 years post burn).

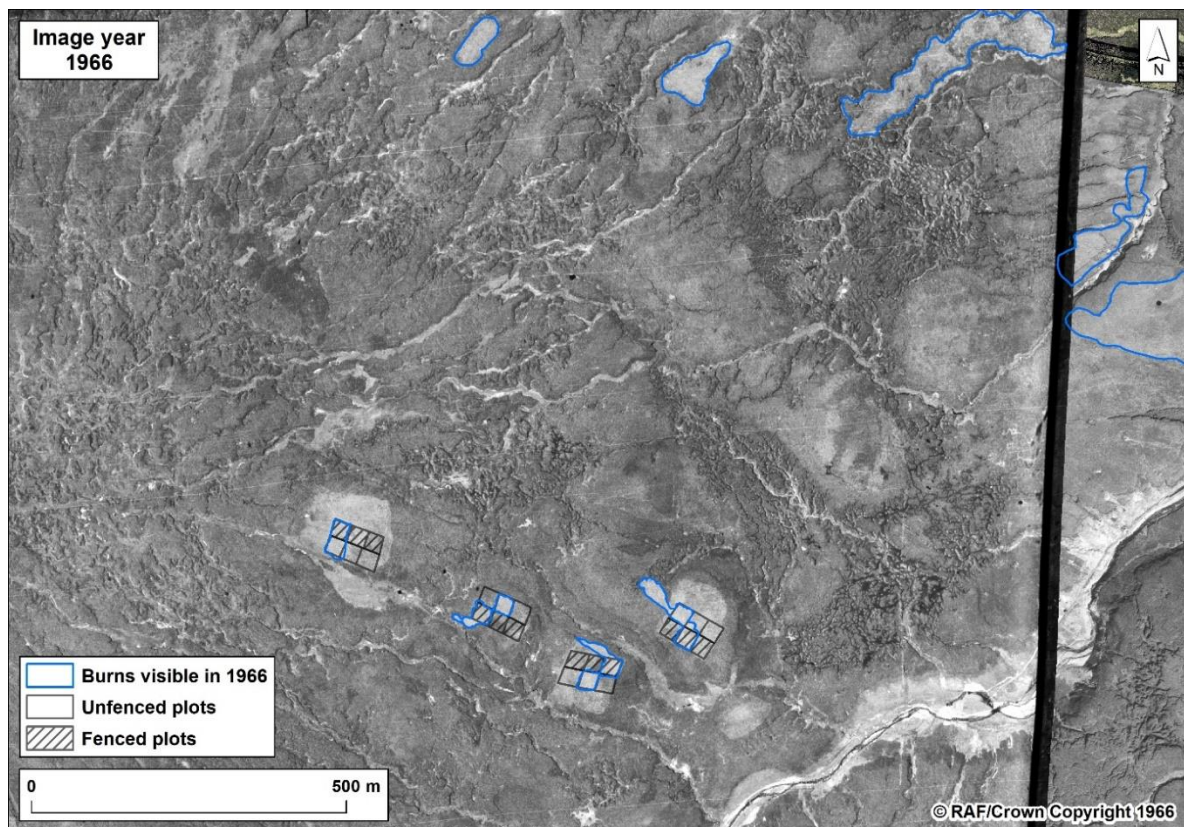


Figure 6 Hard Hill in 1966 showing location of burns undertaken in 1965 inside 10-year plots and burns from other years outside the experimental area.

2.5 Aerial imagery – 1969

It can be seen from the photograph taken in 1969 that no further burning had occurred in the wider area of Hard Hill since 1966 (Figure 7). All burning post-1964 outside the experimental area on Hard Hill is reported to have been confined to the area of Green Burn and Force Burn 3 km south-east (Rawes, 1965). It is important to note, however, that the outline of five of the six burn patches from 1953/1954 (15-16 years post burn) and the five burns from 1956 and 1961 outside the experimental area of Hard Hill (8-13 years post burn) were not discernible from the background vegetation. Combined with observations from the photograph captured in 1966, a good estimate can be obtained for the age of the pre-experimental burn scar visible in Block B in 1954.

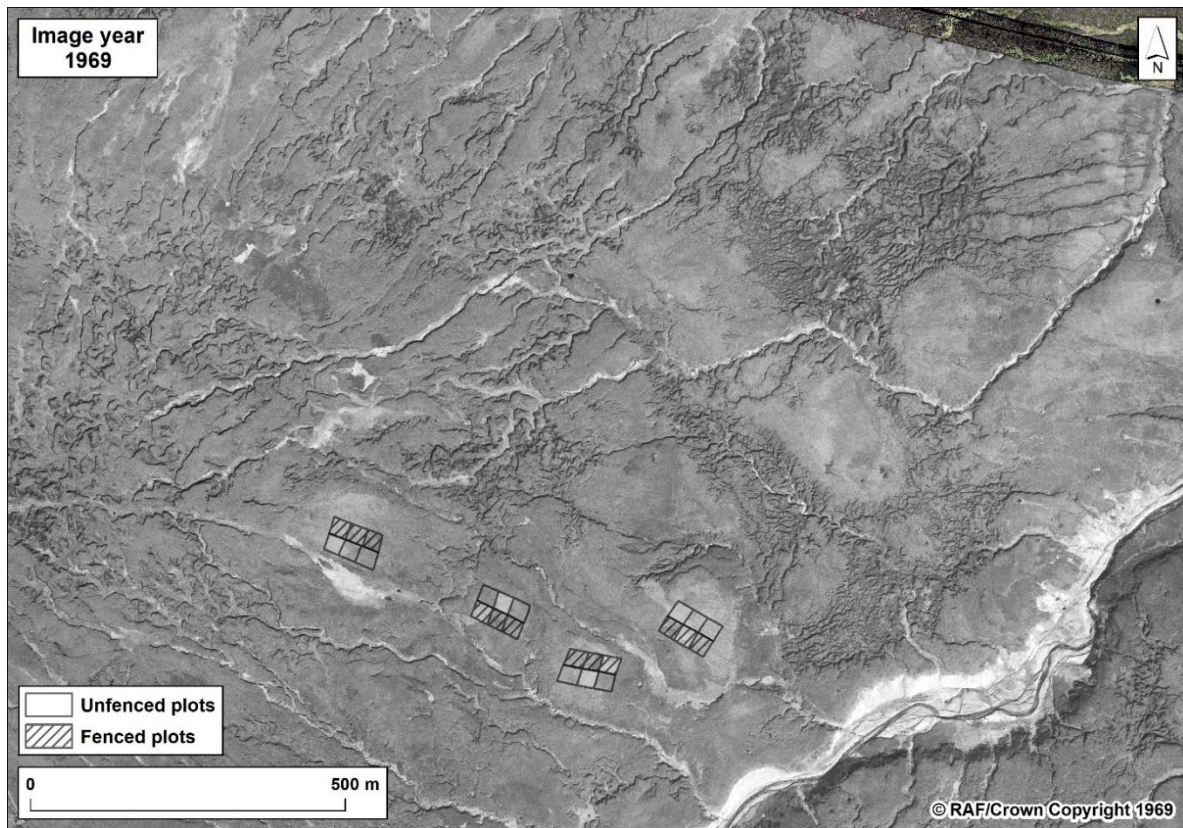


Figure 7 Hard Hill in 1969 showing that no further burning had occurred in the NNR since 1966.

At the plot-level, a number of further important observations become apparent from the high-resolution image captured in 1966.

2.5.1 Erosion features

In Block D, a linear feature is apparent running diagonally through both plots not burned since 1954 in the experiment. This feature is visible in all subsequent aerial imagery (Figure 8), as are several other meso-scale features. From terrestrial laser scanning (TLS), UAV and ground survey these features are revealed to be significant erosion gullies (Clutterbuck, 2015). Interestingly, a ground survey in 1965 reported that the ground layer in the fenced plot that has not been burned since 1954 was “...a honeycomb of tunnels, presumably made by a vole” (Rawes, 1965). In Block A, there is a greater visual contrast in the vegetation in the fenced plot that has not been burned since 1954 when compared with the other plots (Figure 9). From TLS, UAV and ground survey, this plot has been found to contain an erosion feature that is characterised as comprising a near-circular depression in the centre of the plot. These erosion features, and the potential impact that these could have on vegetation (Lindsay, 2010) and hydrology (Daniels et al., 2008), have not been reported nor considered in studies assessing differences between treatments.

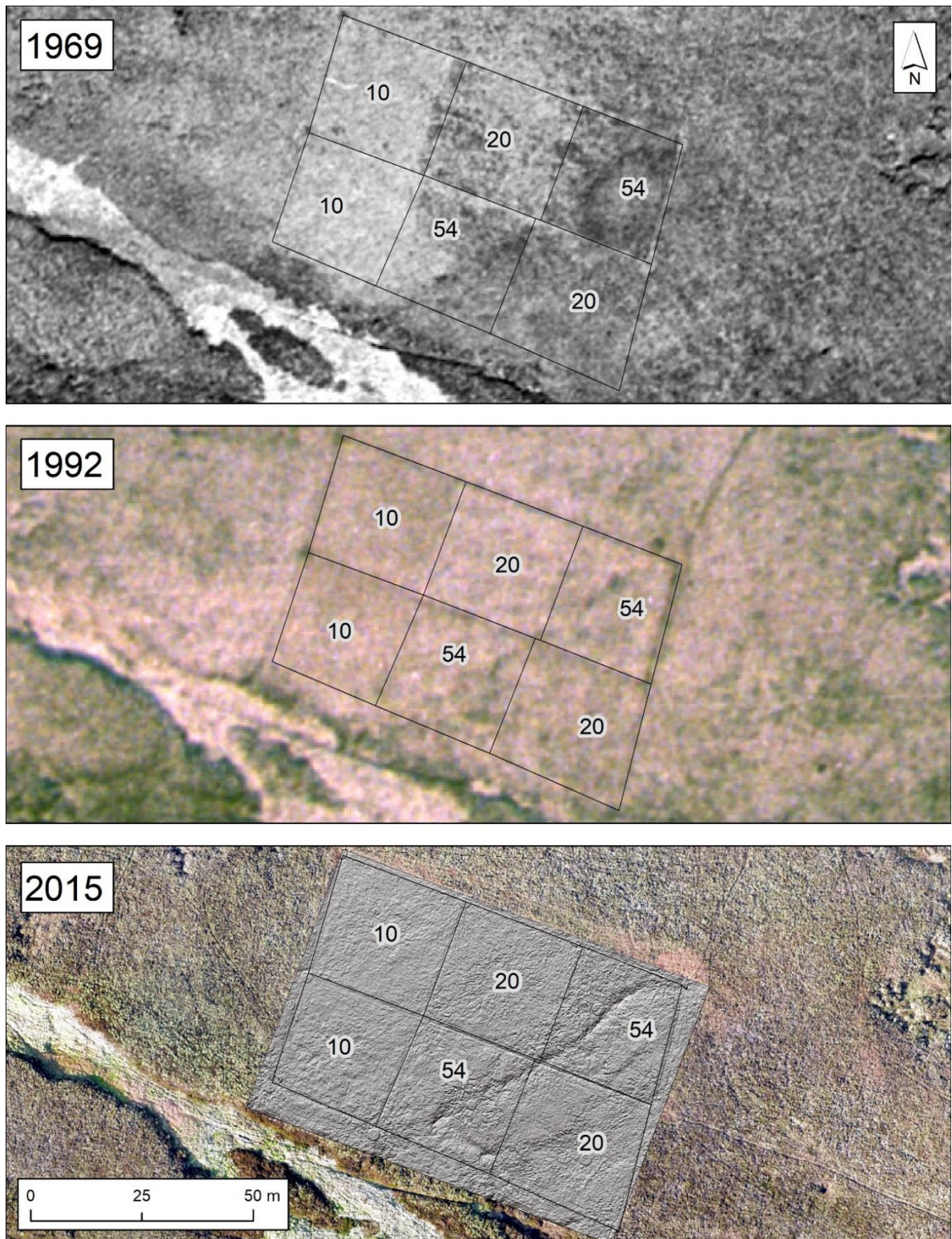


Figure 8 Presence of meso-scale erosion gullies in experimental Block D. The imagery for 2015 shows a model of the peat surface underneath vegetation extracted from TLS survey.

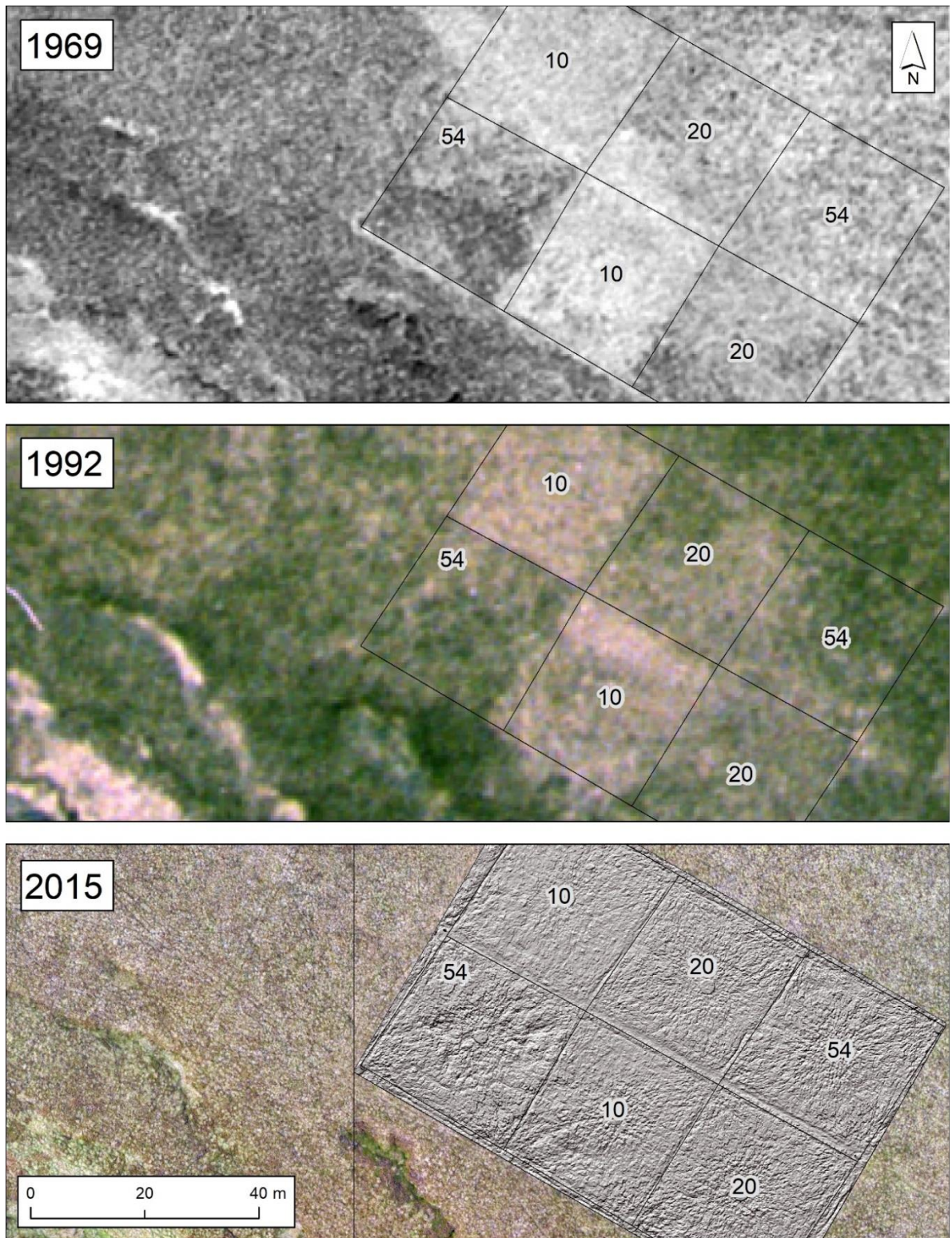


Figure 9 Presence of erosion feature in experimental block A.

2.5.2 Visible persistence of pre-experimental burn scars

In Block B the burn scar visible in 1953 affects four of the component experimental plots (Figure 10). What is compelling is that the outline of this burn scar is visible in imagery captured in both 1969 and 1992.

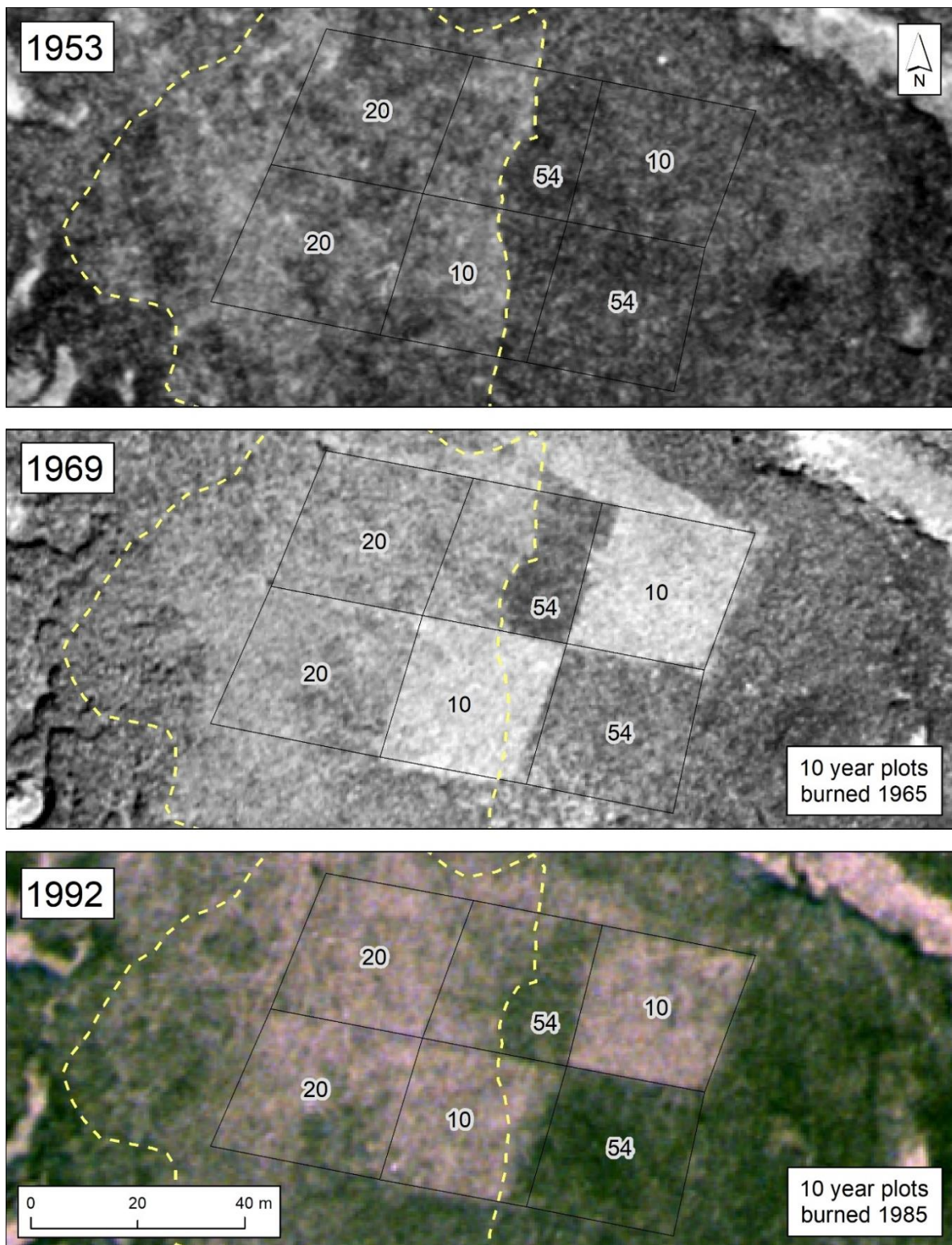


Figure 10 Impact of pre-experimental burn on vegetation in experimental block B.

The impact of burning on vegetation structure is particularly pronounced in a plot that has not been burned since 1954. This plot was burned in its entirety only once during the course of the experiment, and the portion of the plot that had previously been burned 12-15 years prior to the experiment is visually much brighter than the portion that was not burned prior to the experiment. From a ground survey in 1965 *Eriophorum angustifolium* was noted to occur only in the upper (westerly) part of the plot where it was reported as being “...quite concentrated, and plays an important part in the vegetation cover” (Rawes, 1965). The location of *E. angustifolium* noted on the ground coincides with the visual difference visible in aerial photography.

It would seem, therefore, that the difference in vegetation structure in at least one plot, visible 40 years after the experiment started, relates to pre-experimental conditions, not the experimental treatments.

A similar phenomenon is visible in a plot not burned since 1954 in Block A, although the visual contrast between the vegetation is less pronounced in 1992 (Figure 11). This would suggest that the impact of pre-experimental burning on vegetation structure can still be detectable 50-60 years after a fire. Such a possibility is supported by the evidence of identifiable vegetation differences noted between the experimental plots and the original reference plots even 60+ years after the start of the experiment (Lee et al., 2013; Noble et al., 2018).

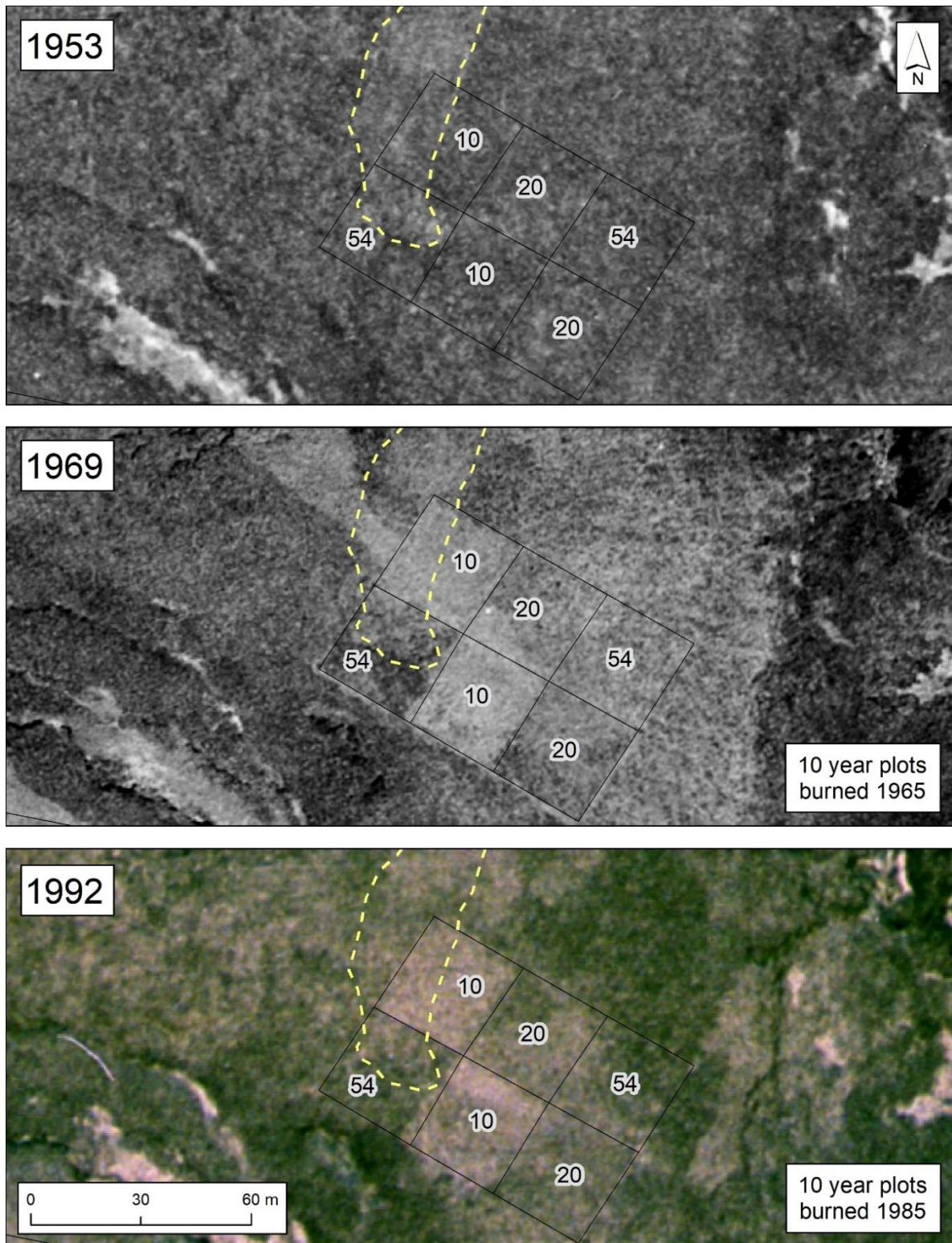


Figure 11 Impact of pre-experimental burn on experimental block A.

2.6 Aerial imagery – 1992

At the time of writing it has not been possible to identify any aerial photography covering Hard Hill between 1969 and 1992. However, the brighter appearance visible in the imagery of the vegetation in the 10-year plots in Blocks A-C indicates that the burning of these plots in 1985/6 did indeed take place (Figure 12).

It is not clear, though, why four new burn scars are evident in the vegetation outside of the experimental plots.

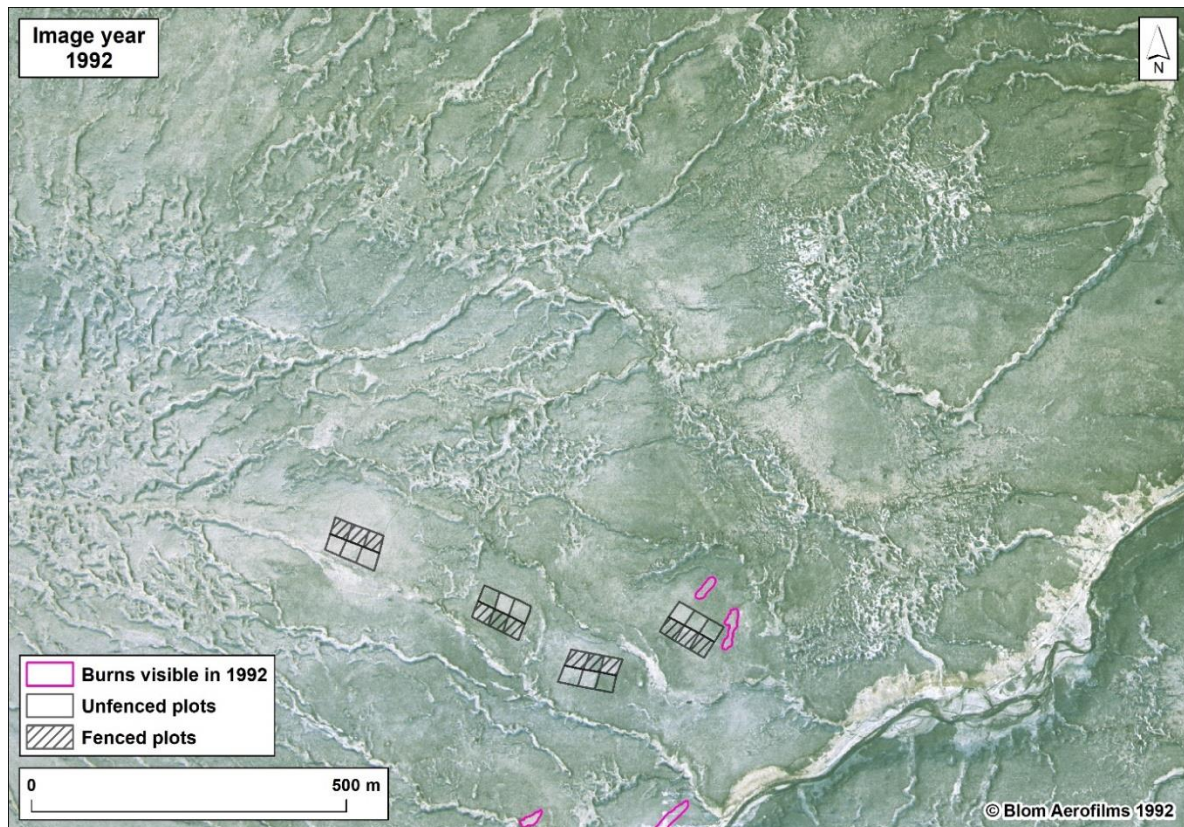


Figure 12 Hard Hill in 1992 showing location of burns undertaken in 1985/6 (inside 10-year plots and outside).

2.7 Aerial imagery – 1995

It can be seen from the photograph taken in 1995 that both the 10- and 20-year plots were burned in 1994/1995 (Figure 13). It is also evident that no further burning had occurred in the wider area of Hard Hill since 1992, and this has remained the case to present day (section 2.8). Certain other issues are, however, evident from the 1995 imagery.



Figure 13 Hard Hill in 1995 showing location of burns undertaken in 1994/5 (inside 10- and 20-year plots).

2.7.1 Inconsistent burn extents

In addition to the burns undertaken in the plots in 1965, the photography from 1995 reveals further inconsistent burning in Block D. In 1965 the 10-year fenced plot was not burned in its entirety, and the fire from the 10-year grazed plot spread into the grazed plot not burned since 1954 (see Figure 14). In 1995, 15-20% of the same grazed plot not burned since 1954 was burned by fire from the 20-year grazed plot, while the 20-year fenced plot was not burned in its entirety. This inconsistency is still visible in 2002 (Figure 14).

From 2002 onwards, the extent of burns in the plots appears far more consistent, perhaps indicating a different style or approach to burning.

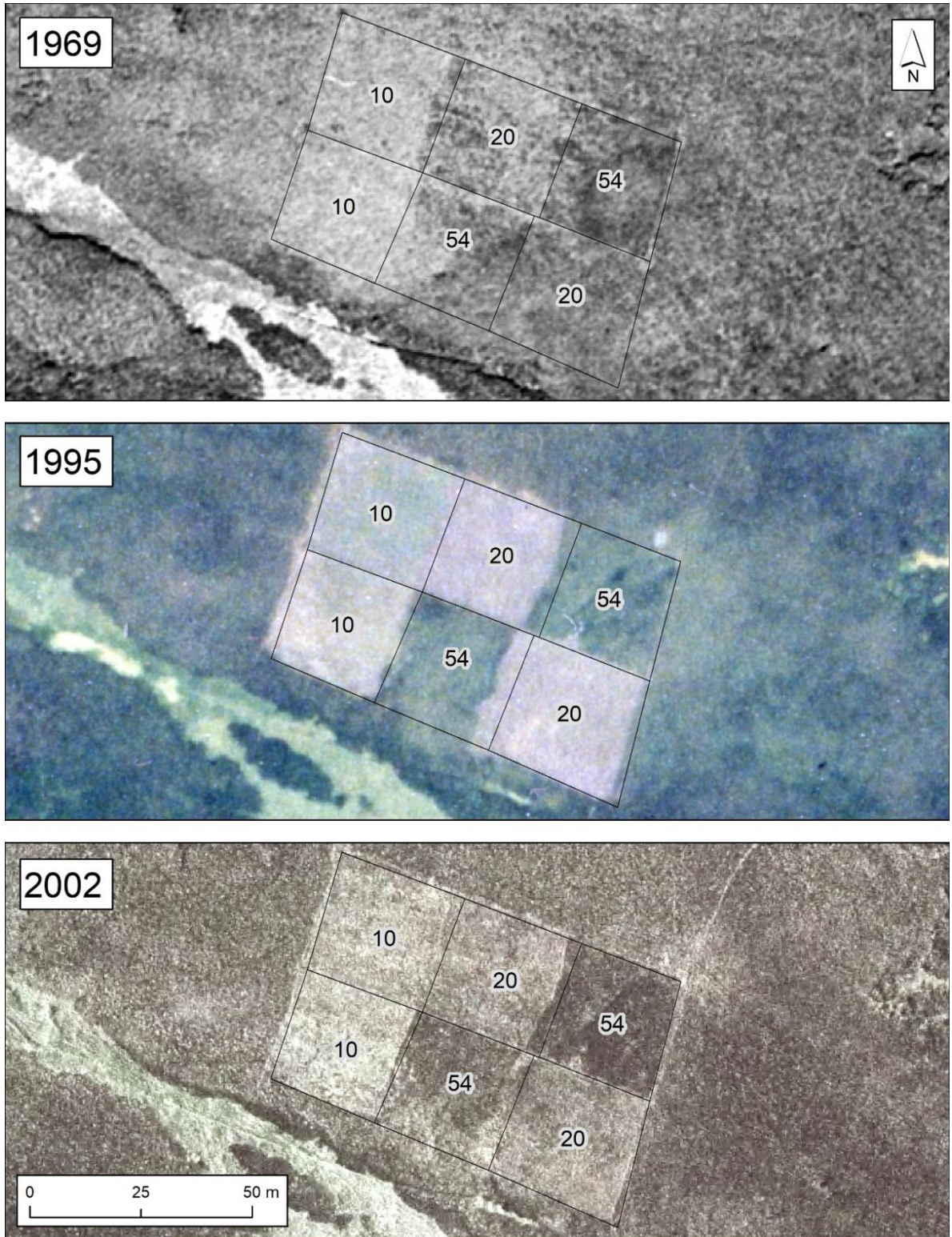


Figure 14 Inconsistent burn extents in experimental block D.

2.8 Aerial imagery – 2002-2018

In imagery for the years 2002-2018 it is evident that burning was constrained solely to the experimental plots (Figures 15-18). The cycle of burn rotations (Table 2) was undertaken in 2007 (10-year plots) and 2017 (10- and 20-year plots).

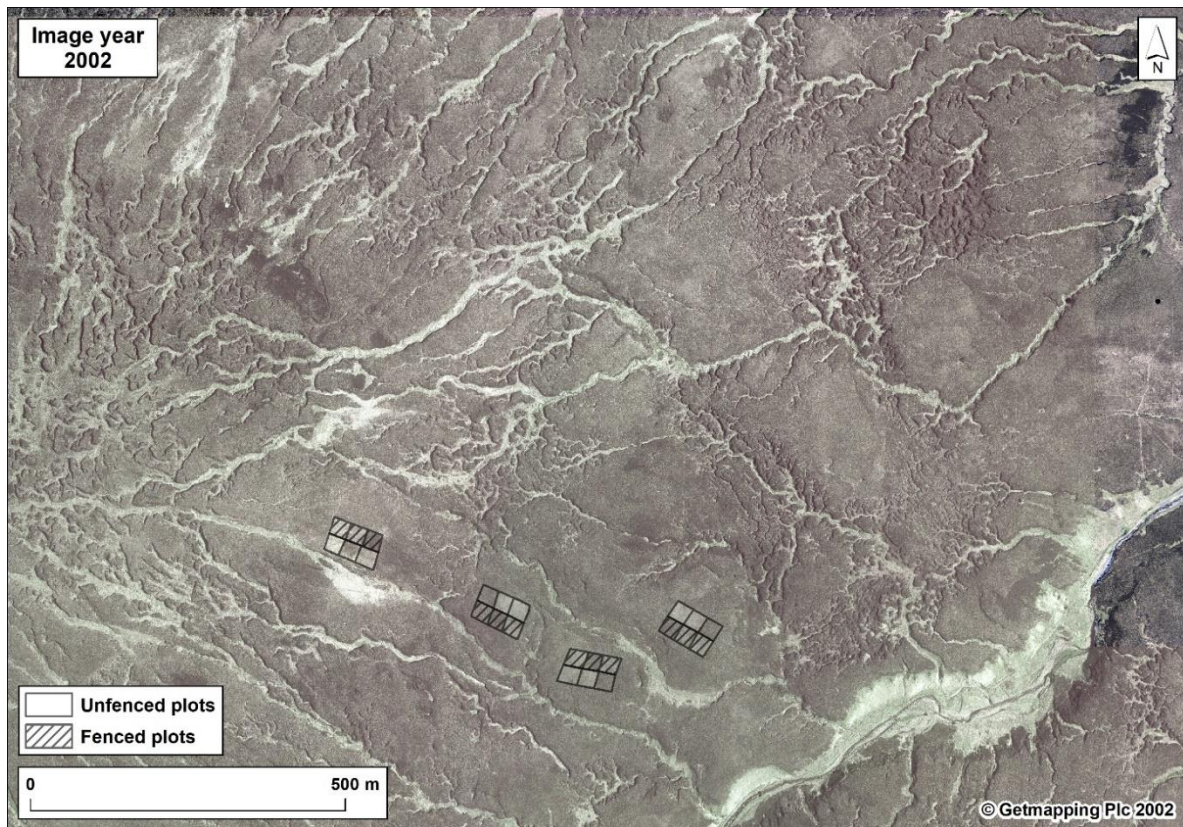


Figure 15 Hard Hill in 2002 showing location of burns undertaken in 1994/5 (inside 10- and 20-year plots).

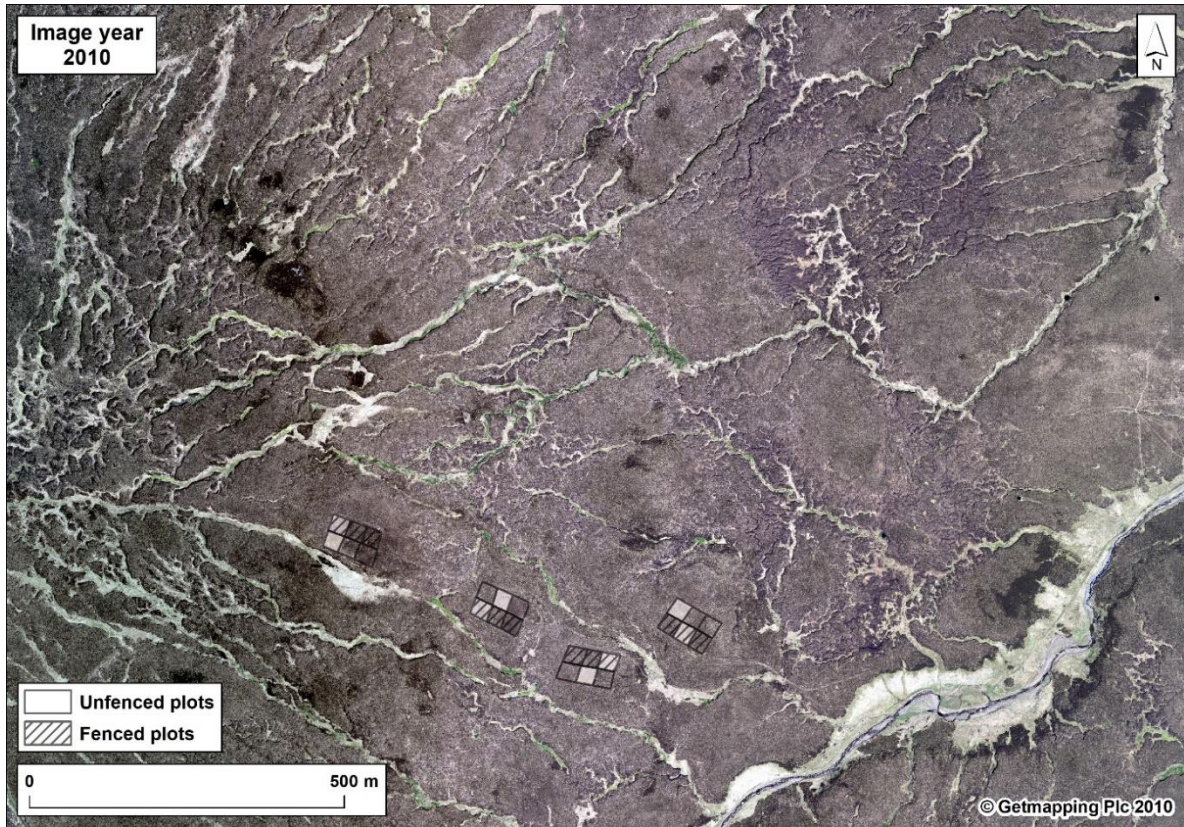


Figure 16 Hard Hill in 2010 showing location of burns undertaken in 2007 (inside 10-year plots).

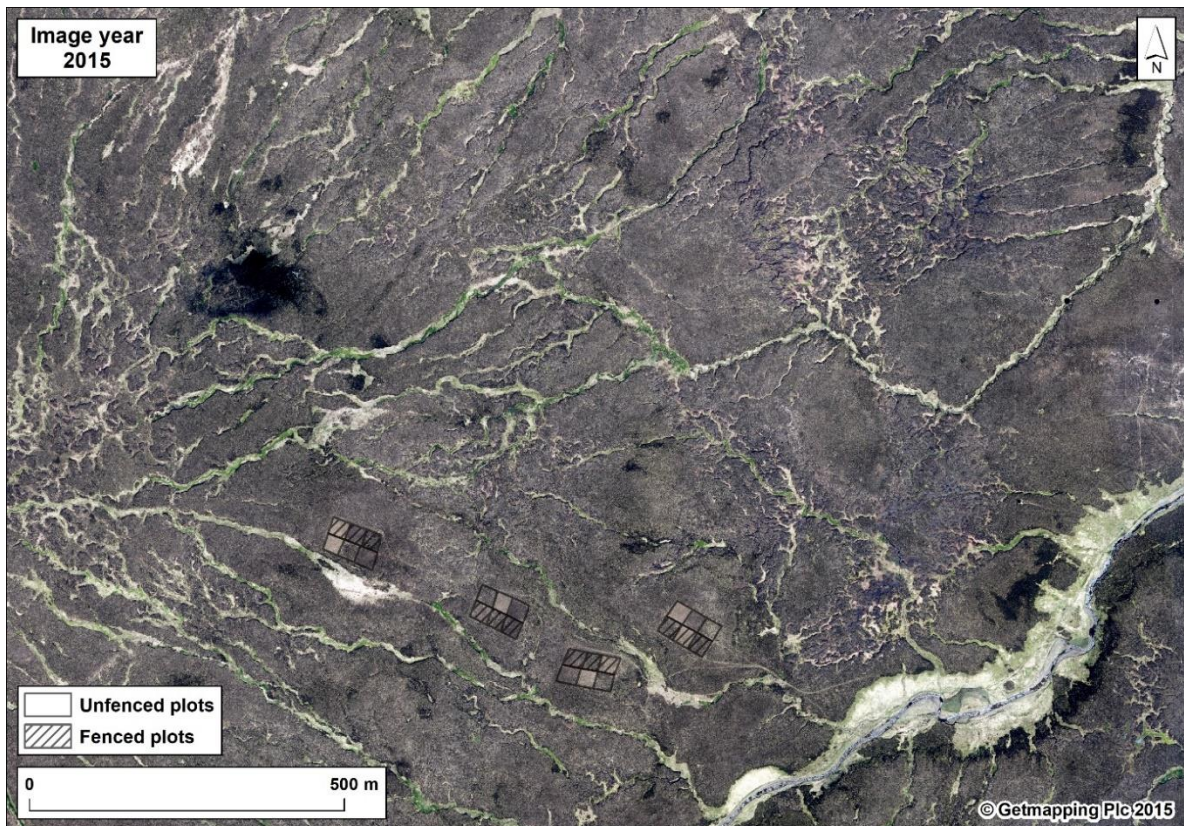


Figure 17 Hard Hill in 2015 showing location of burns undertaken in 2007 (inside 10-year plots).

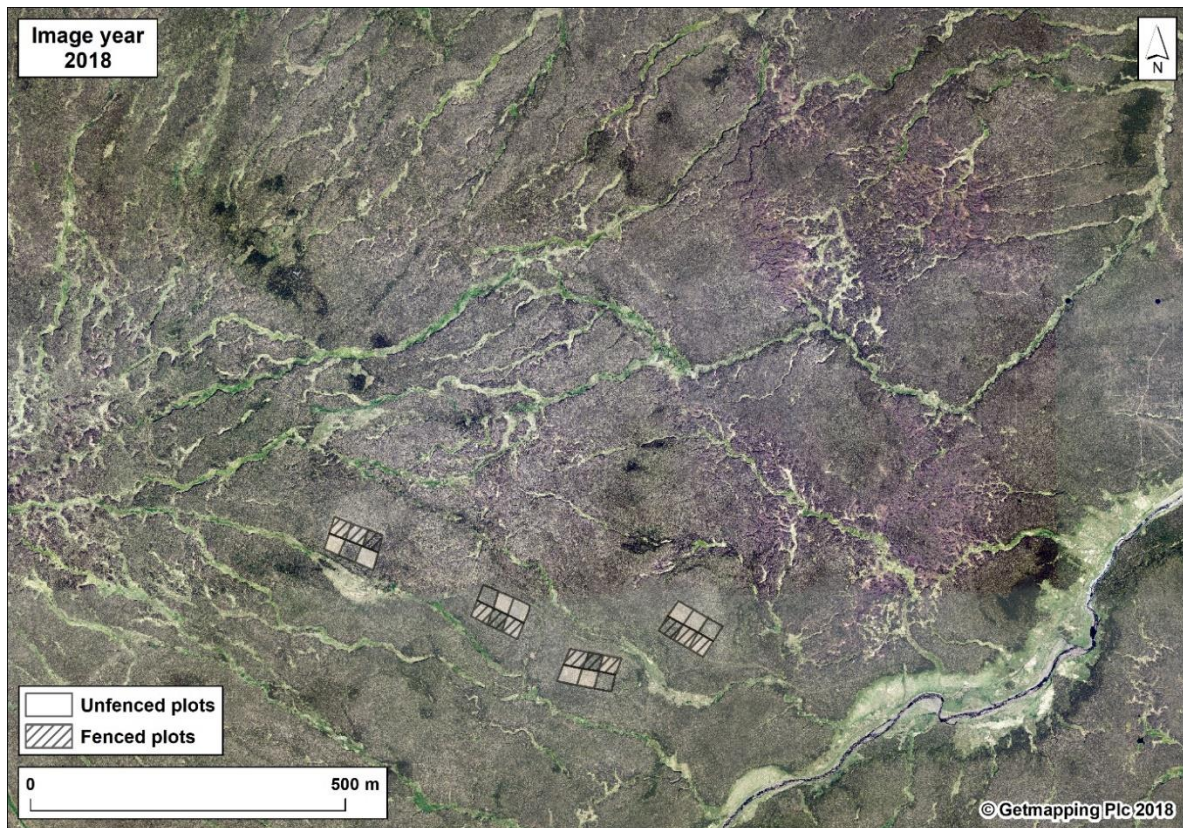


Figure 18 Hard Hill in 2018 showing location of burns undertaken in 2017 (inside 10- and 20-year plots).

This overall pattern of burning history, markedly different from the generally assumed pattern in much that has been published, raises important questions about interpretation of results and appropriate analytical approaches. In considering differences in productivity between differing parts of Moor House, Forrest and Smith (1975) noted:

“The between-site variation that does exist is largely due either to the existence of a seral state produced by management factors such as burning, or to differences in species composition resulting from differences in edaphic factors, in particular wetness.”

Having highlighted anomalies concerning the true seral state of various treatment plots, the present report also now considers the second factor highlighted by both Forrest and Smith (1975) and Rawes and Hobbs (1979) – namely variations in ‘wetness’, as determined at least in part by the slope of the ground between and within the four experimental blocks.

3 Gross morphology and micro-relief of the experimental blocks and plots

3.1 Slope

Determination of slope from raster data (digital elevation models; DEMs) is a relatively simple task using GIS. The slope algorithm compares the elevation value of each pixel in the raster dataset to the elevation value of all adjacent pixels and determines the largest difference in height. This height difference provides the maximum slope angle for that pixel (calculated as change in height over distance, where distance = pixel size). The spatial resolution of the raster data (i.e. pixel size) will therefore have a significant impact on the slope values determined.

Digital elevation models derived from UAV imagery (<2 cm resolution in this study) provide wide context of the landscape with which to determine slope, but the elevation model includes vegetation and other surface objects (digital surface model; DSM). As the 10- and 20-year plots were burned in the spring of 2017, the difference in vegetation height in these plots compared to the vegetation in the plots not burned since 1954 is clearly visible in the DSM derived from UAV data even at the landscape scale (Figure 19). Slope derived from the UAV DSM data is therefore not consistent or comparable across the experimental blocks because the values are confounded by differences in vegetation height.

To understand the general slope of the experimental blocks and plots it is therefore more appropriate to model slope from the elevation of the terrain – namely the ground surface beneath the vegetation cover. Digital terrain models (DTMs) have been derived from TLS data for all blocks on Hard Hill (output at 2.8 cm resolution) following digital removal of the vegetation layer (Clutterbuck, 2015). These data enable the slope of the peatland surface to be modelled in ultra-high resolution, but at this scale the analysis will determine the slope of microtopographic features and therefore provides more of a ‘roughness’ index of the peat surface rather than the general slope of the peatland.

DTMs derived from airborne Lidar data have several advantages over TLS data. Firstly, the coverage of airborne capture is significantly greater than that from TLS, thereby providing a far more efficient approach to assessing landscape-scale topography. In addition, the laser beam diverges with distance from the aircraft and therefore the footprint of each laser ‘beam’ on the ground is several orders of magnitude larger than the footprint of a laser beam from a TLS. The height recorded by airborne Lidar is therefore the mean value of height for a far wider area than that assessed by TLS, and effectively removes microtopographic variation.

3.1.1 Slope across experimental blocks

A DTM for Hard Hill derived from airborne Lidar captured in 1999 (2 m resolution) was obtained from the Environment Agency (EA). Large erosion features and streams surrounding the experimental blocks are clearly defined in these Lidar data, yet the erosion features in block D evident in the UAV derived DSM are not visible (Figure 19). Slope determined from airborne Lidar would therefore appear to provide the best representation of the general slope of the terrain.

The mean slope of the terrain determined from airborne Lidar for Hard Hill increases progressively uphill (Blocks A to D) from 4.9° in Block A to 7.3° in Block D (Table 3; Figure 20). The range of slope values also increase uphill and relate to a notable doubling of maximum slope from 9.0° in Block A to 18.0° in Block D (Table 3).

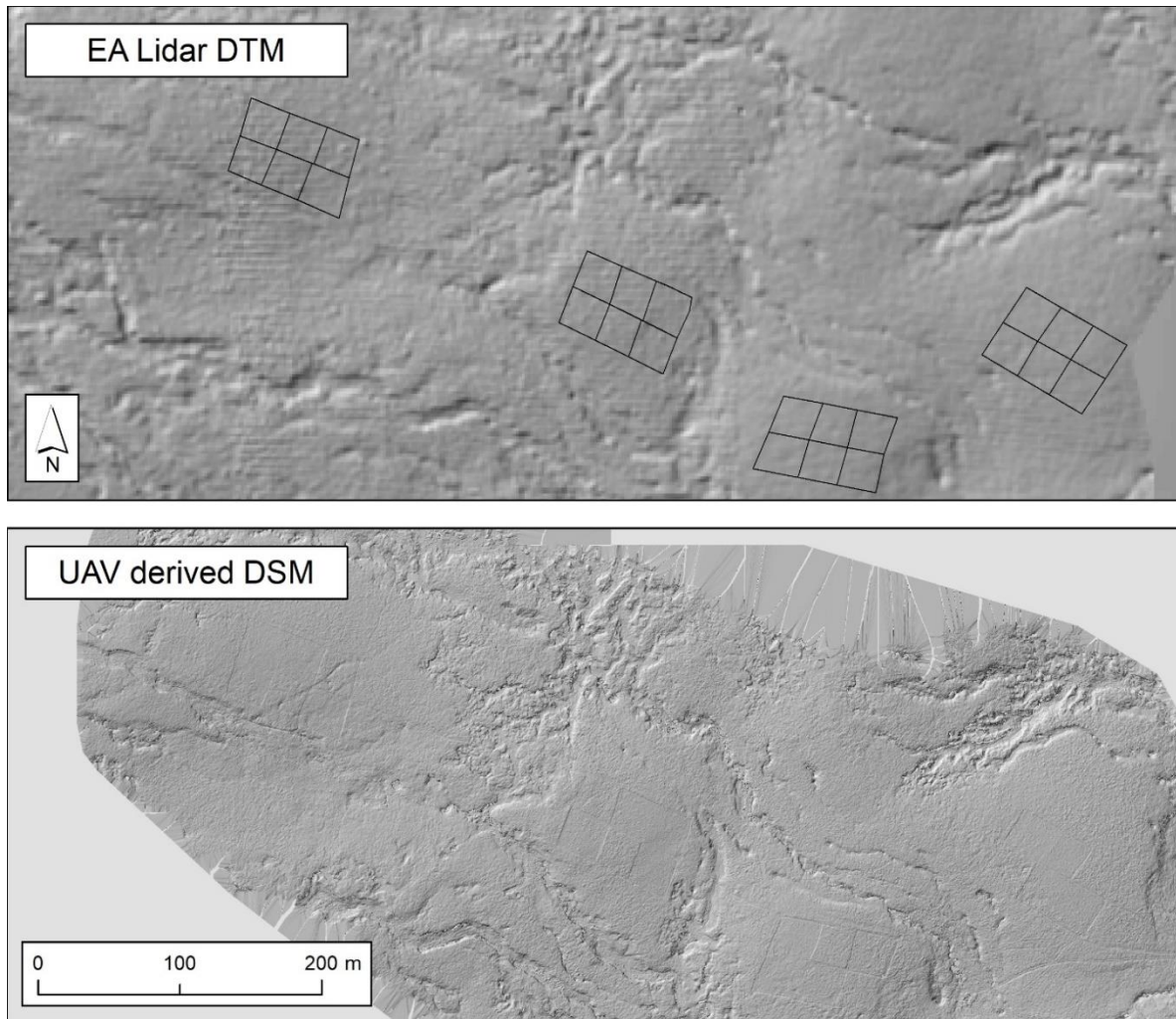


Figure 19 Topography of Hard Hill visible in airborne Lidar (DTM) and UAV derived DSM (hillshade view shown).

Table 3 Slope of terrain in experimental blocks on Hard Hill derived from airborne Lidar (DTM).

Block	Mean slope (°)	Maximum slope (°)	SD
A	4.90	9.02	1.36
B	5.25	11.73	1.71
C	5.99	16.11	1.94
D	7.29	18.02	2.21

These data suggest that the rate of drainage and surface runoff increases uphill. Block A might therefore be expected to hold water for longer than Block D, and it is possible that the distinct differences referred to earlier in vegetation composition recorded between the experimental blocks in 1961 – specifically in *Calluna vulgaris*, *Rubus chamaemorus*, *Eriophorum angustifolium* and *Sphagnum* spp. (Hobbs, 1984) – relate to a difference in hydrology between the blocks.

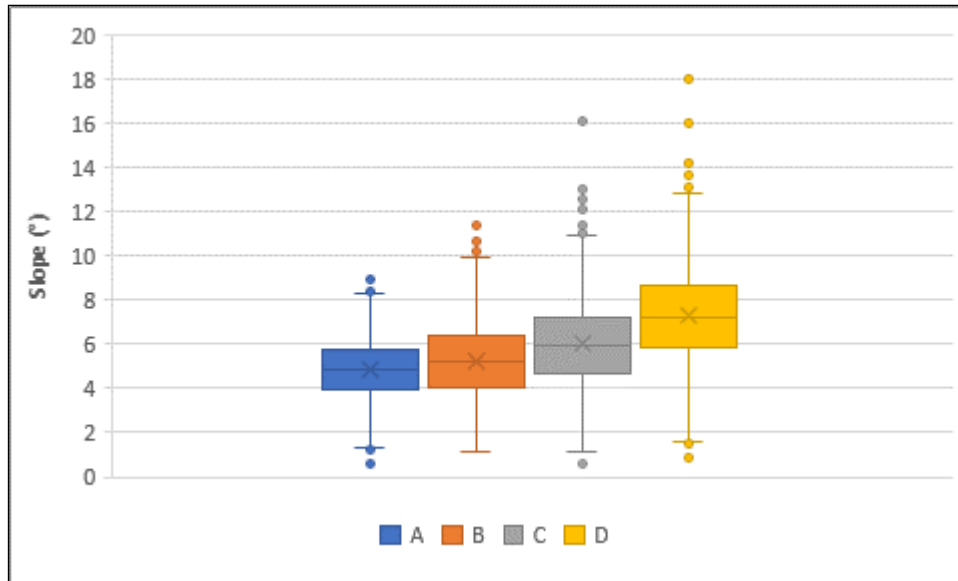


Figure 20 Slope of the terrain across experimental blocks on Hard Hill derived from airborne Lidar (DTM).

3.1.2 Slope across plots

The increasing trend in mean and maximum slope of the terrain uphill is also evident at plot level (Figure 21), but there is an additional trend in slope noticeable across the treatments. Grouped by burn treatment, the 10-year plots have the lowest mean slope in three of the blocks (A, C and D) and the plots not burned since 1954 have the highest mean slope in three slightly different blocks (A, B and D; Figure 21).

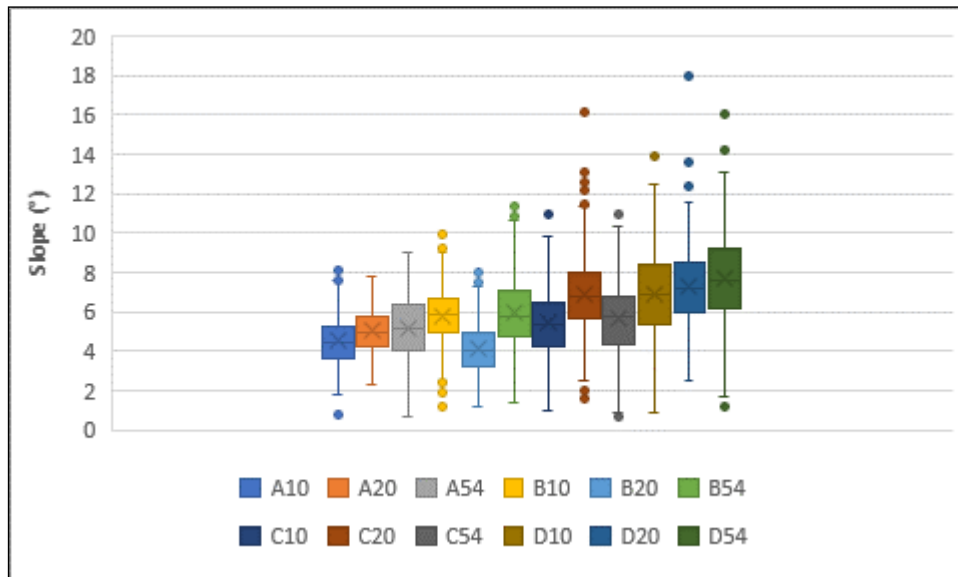


Figure 21 Slope of the terrain across plots (grouped by burn treatment per block) on Hard Hill derived from airborne Lidar (DTM).

The present study has already highlighted anomalies concerning both the meso-scale relief and post-fire seral state of various treatment plots, but can also point to differences in slope and thus potential differences in hydrological character within blocks and between treatment plots within these blocks. It is therefore worth highlighting the observations of Rawes and Hobbs (1979) concerning the variability displayed by vegetation stands across Moor House as a whole:

“Forrest & Smith (1975) examined the differences in primary production of seven blanket bog sites at Moor House, all within 2.5 km of each other and at similar altitude, and found a two-fold variation between the extremes, the gradient of decreasing production being correlated with increasing wetness. Thus the blanket bog vegetation cannot be assumed to be homogeneous, and any change following treatment must be related to the site concerned.”

3.2 Effect of micro-relief on slope values

At the fine scale of data measurement capable of being influenced by the micro-relief (microtopography) of the bog surface, slope values take on another meaning. A very flat micro-relief will generate a fairly uniform set of values whereas a highly structured micro-relief with much vertical structure will generate composite data that indicate higher slope values. This is because individual tussocks or hummocks will tend to have steeper slopes on all sides compared with a more level micro-relief. The composite slope values will thus tend to be greater for a tussocky or hummocky terrain than for a flat terrain.

To explore variations in slope at the finer scale of plot microtopography, each individual plot was examined using the TLS-derived DTMs. At the scale of vertical resolution using TLS (here 2.8 cm), depressions in the peat surface created by persistent footfall since 1954 are prominent features in the data, particularly around edges of plots and along the fence lines (Clutterbuck, 2015; Figure 22), and will affect micro-scale determination of slope in these areas. Artefacts in DTM height data also occur directly below the scanner/tripod location. For consistent assessment of microtopographic influence on small-scale slope values, elevation data in the DTM were examined within a 10 m radius circle in the approximate centre of each plot but excluding the area below the scanner (1.5 m radius circle; Figure 22). This area of assessment also excludes areas impacted by inconsistent burning (section 2.7.1).

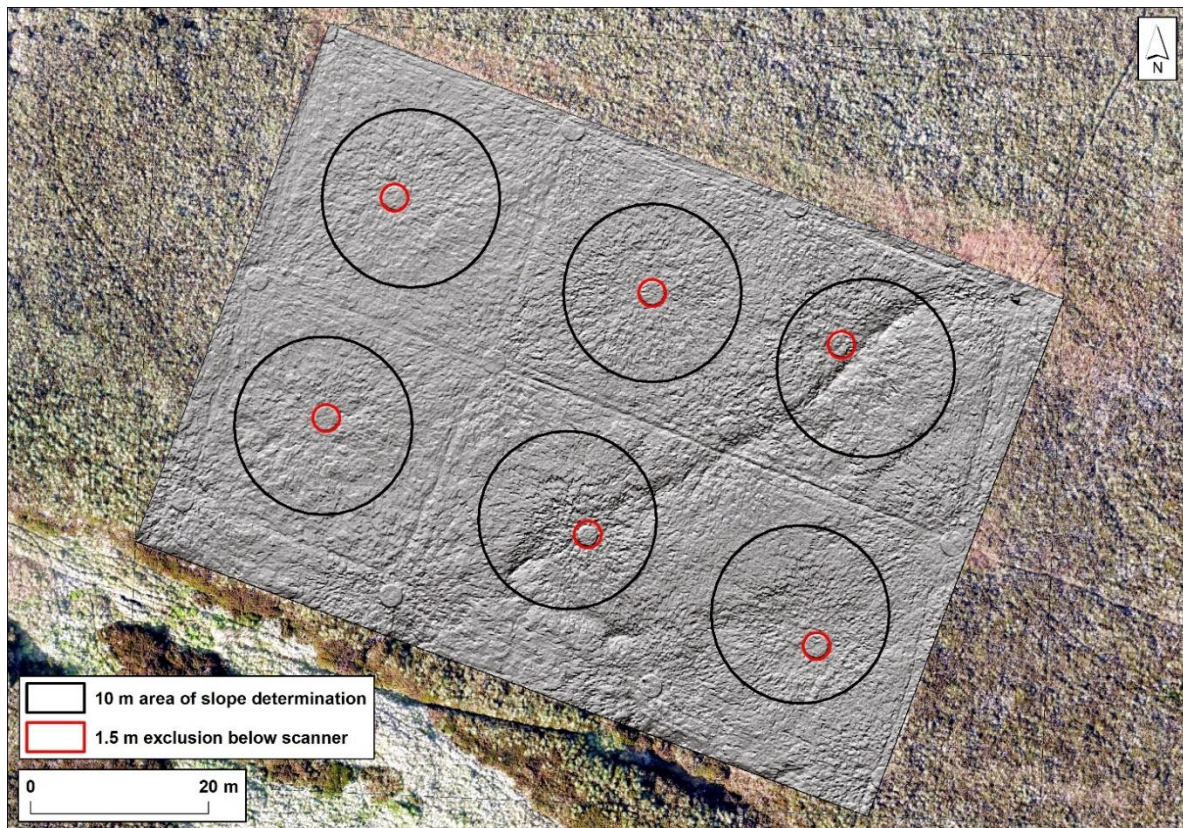


Figure 22 DTM derived from TLS survey for block D showing area assessed for plot level slope analysis (note the visible depressions in the peat surface created by persistent footfall since 1954, particularly around edges of plots and along the fence lines).

Observations of a trend in terrain slope for plots grouped by treatment type are more marked in the analysis of microtopographic slope from the TLS DTM data than is the case for meso-scale slope values obtained from Lidar data. With the exception of the fenced section of Block B, the mean micro-scale slope of plots burned on 10-year intervals is lower than the mean micro-scale slope of all other plots in all blocks (Table 4). The variation in micro-scale slope (SD) in the plots burned on 10-year intervals is also lower than the variation in micro-scale slope in all other plots in all blocks, including in the fenced section in Block B. In addition, in Blocks A, B and D, the mean slope of plots not burned since 1954 is higher than the slope of plots burned on 20-year intervals in both fenced and grazed areas in each block (Table 4).

While the TLS-derived DTM data have thereby revealed significant meso-scale erosion features in nearly half of the blocks not burned since 1954 (section 2.5.1), the micro-scale slope analysis from the TLS data also highlights a consistent difference between treatments at the scale of surface micro-relief. Microtopographical variation (inferred from the mean and SD of slope in Table 4) in all plots not burned since 1954 is greater than the micro-scale variation found in all plots burned on 10-year cycles and greater than the micro-scale variation in the majority of blocks burned on 20-year cycles. This picture of structural variation suggests that, for the regularly burnt plots, repeated burning has perhaps maintained the bog surface in something similar to a state of arrested development, a state not much different from the relatively flat surface punctuated by low tussocks which, given Forrest's (1961) description of the 1954 fire, may have dominated in all four blocks at the start of the experiment.

Table 4 Mean (\pm SD) slope determined for individual plots on Hard Hill derived from TLS DTM (green and red indicate lowest and highest mean values of slope respectively by fenced (F) and grazed (G) areas).

Plot	Block A	Block B	Block C	Block D
10 F	14.7 \pm 9.9	15.0 \pm 10.3	12.7 \pm 8.7	12.0 \pm 7.7
20 F	17.6 \pm 11.5	14.5 \pm 9.8	18.5 \pm 12.0	16.1 \pm 10.5
54 F	17.9 \pm 11.7	16.1 \pm 10.9	17.2 \pm 11.3	17.8 \pm 11.7
10 G	11.1 \pm 7.7	13.5 \pm 9.2	11.9 \pm 7.9	12.9 \pm 8.3
20 G	16.3 \pm 10.7	15.6 \pm 10.5	17.8 \pm 11.7	16.0 \pm 11.0
54 G	17.3 \pm 11.5	17.2 \pm 11.2	16.8 \pm 11.2	17.9 \pm 12.5

3.3 Drainage patterns

Having identified the presence of erosion features within the experimental plots, the potential impact of these features on hydrological processes within the plots was investigated. Surface-water flow was modelled from the airborne Lidar DTM, the UAV derived DSM and the TLS-derived DTM using the hydrology tools in ArcGIS. Although the erosion feature in Block D is not visible in the airborne Lidar data, the surface flow patterns derived from these data appear to align with a short section of the feature in the NE corner of the fenced plot not burned since 1954 (Figure 23). This alteration of flow path is also visible in the flow modelled from the UAV-derived DSM, but is far more pronounced in the flow modelled from the fine-scale DTM derived from the TLS (Figure 24).

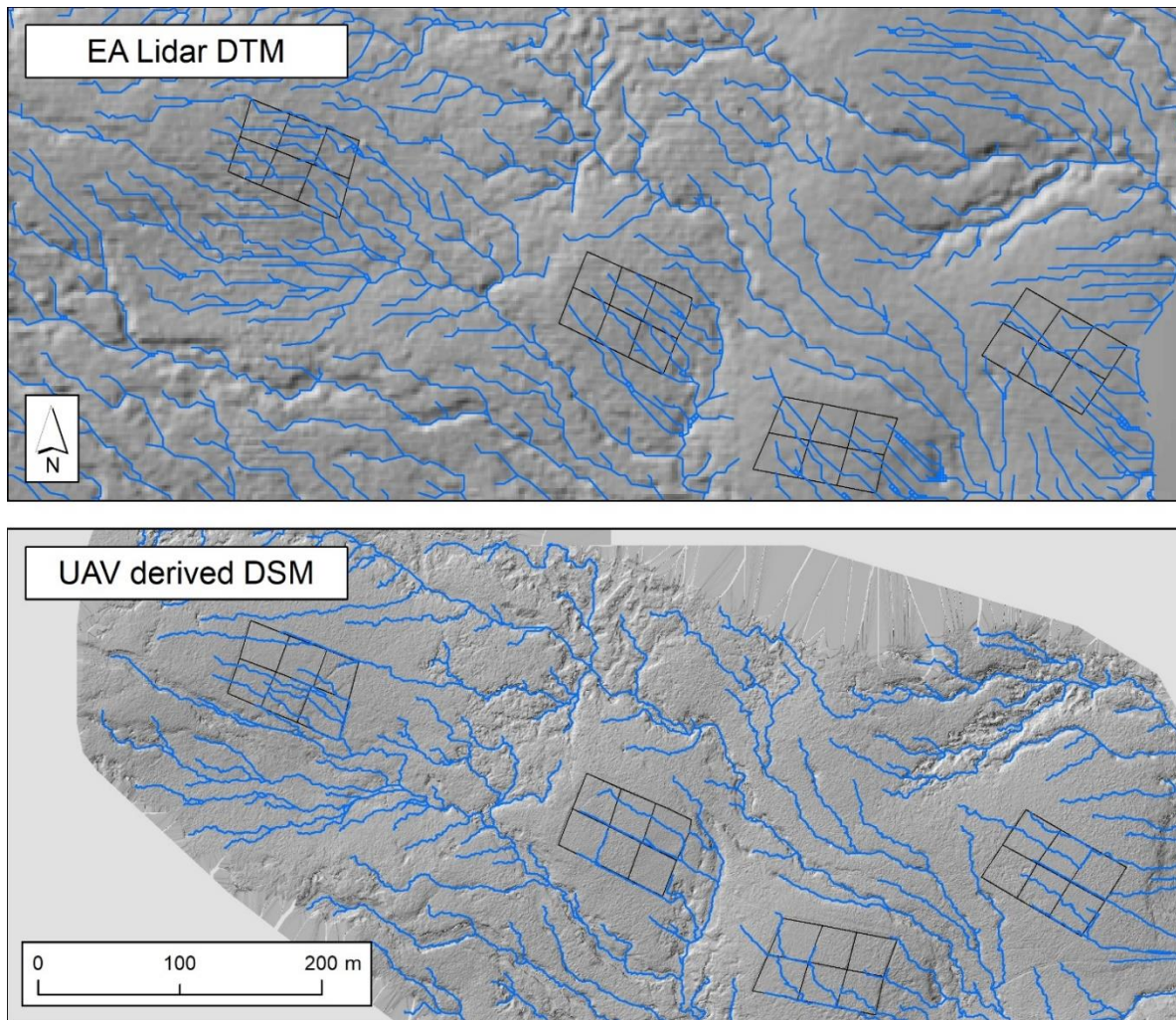


Figure 23 Surface water flow modelled for Hard Hill from airborne lidar DTM and UAV derived DSM data.

Hydrological modelling of the DTM derived from the TLS predicts that downslope surface flow will tend to be intercepted and run along almost the entire length of the erosion feature in the fenced plot not burned since 1954 (Figure 24). The same interception of flow is predicted further along the erosion feature in the grazed plot not burned since 1954, but these two flow paths do not connect. It appears that the break in flow is caused by a greater impact from the depressions caused by footfall along the fence in intercepting surface flow (Figure 24). The interception of surface flow by depressions caused by footfall is evident in all blocks particularly along the fence lines and around the edges of most plots (Figures 23 & 24).

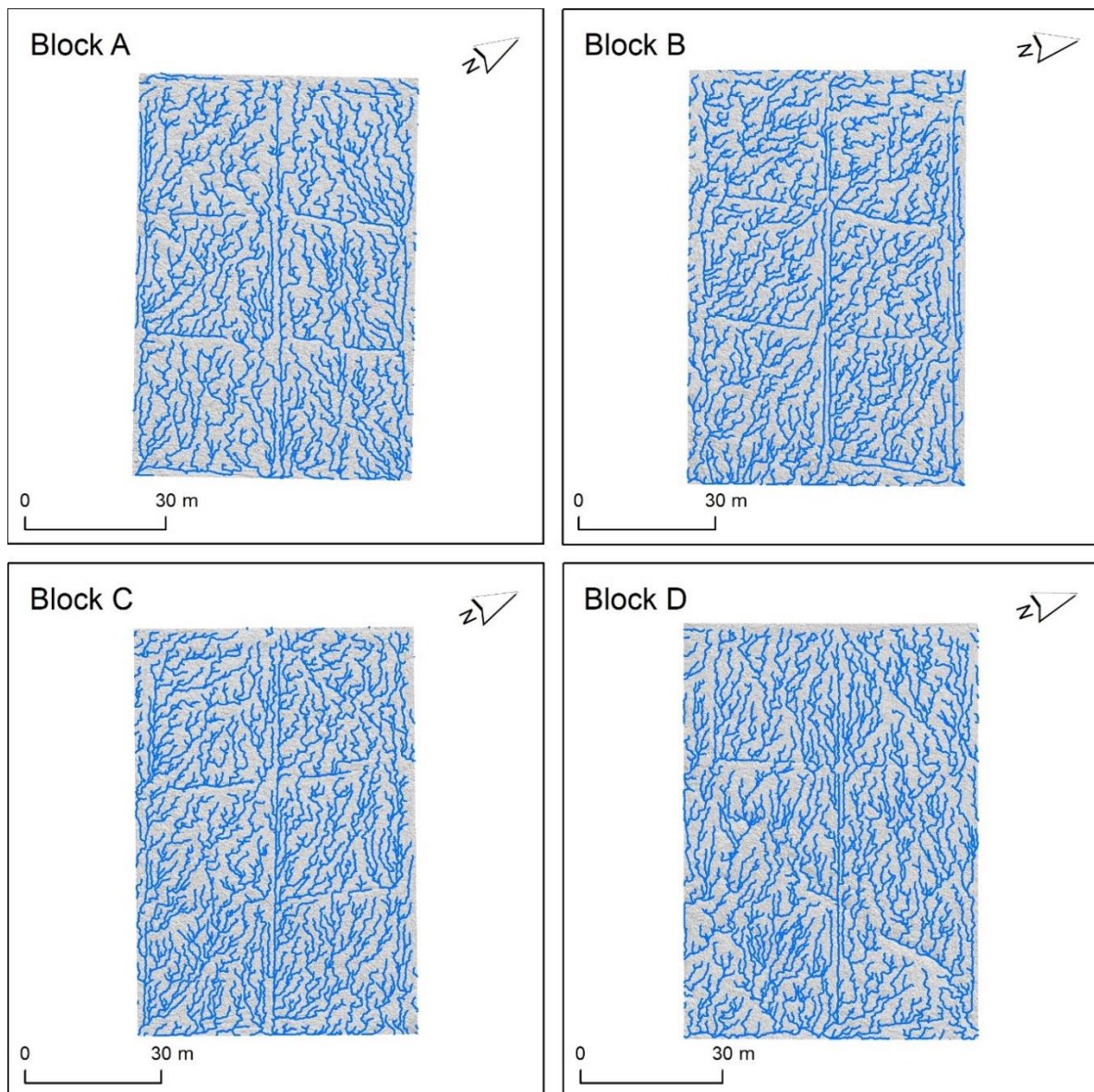


Figure 24 Surface water flow modelled for experimental blocks on Hard Hill from TLS derived DTM data (each block oriented approximately uphill).

3.4 Peat depth

Peat depth in each experimental plot and two additional plots surveyed outside but close to Block D (see Figure 25 & section 4.2.2) was measured using connectable steel rods 50 cm in length and 6 mm in diameter. Measurements were taken in the corners (on the intersection of adjoining plots if appropriate) and in the centre of each plot. Peat depth measurements were interpolated using a spline algorithm in ArcGIS (Figure 25) and the mean interpolated depth determined for each plot (Table 5).

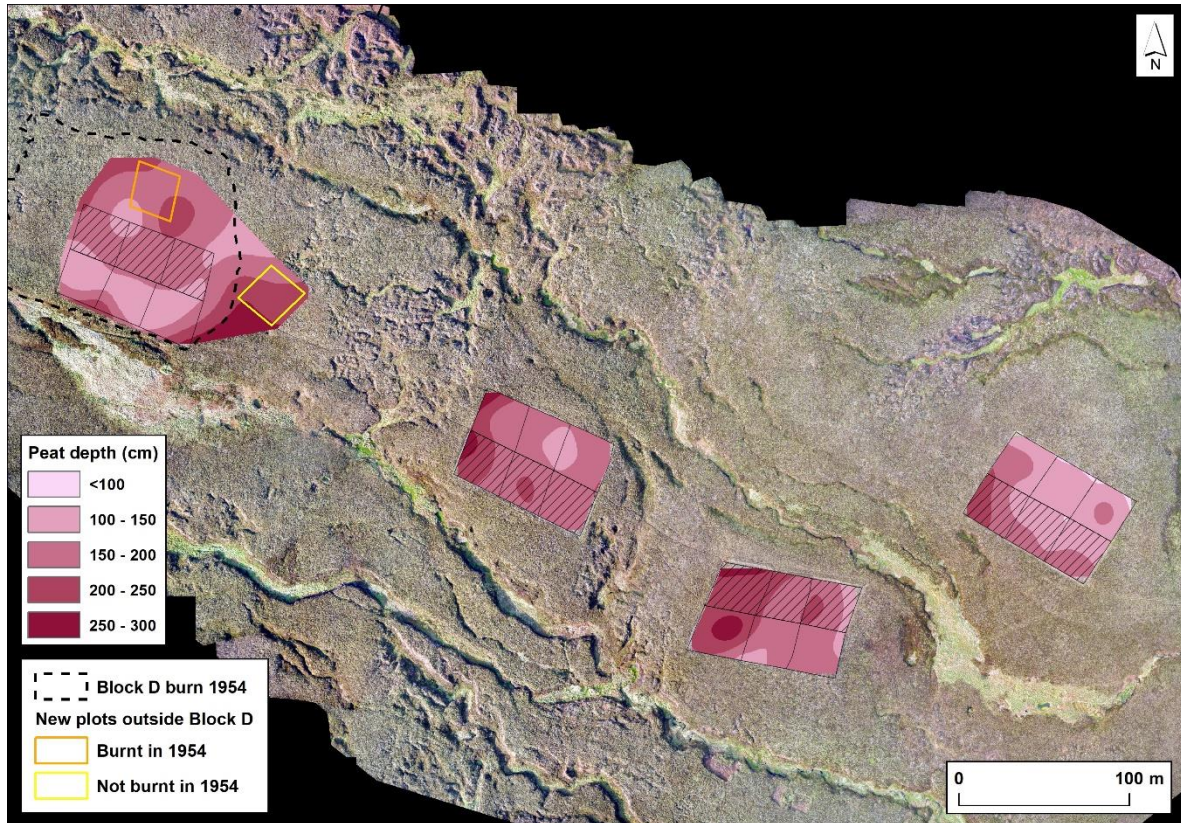


Figure 25 Peat depth across experimental blocks on Hard Hill (location of two additional plots surveyed in 2019 shown).

Table 5 Peat depth across experimental blocks on Hard Hill.

Block	Min measured depth (cm)	Max measured depth (cm)	Range in depth (cm)	Mean interpolated depth (cm)	SD
A	94	212	118	144.7	28.6
B	111	279	168	194.2	34.0
C	149	289	140	182.7	28.1
D	111	262	151	157.4	28.4

Peat depth can be seen to vary considerably across the Hard Hill blocks given that a difference of 195 cm was determined between the lowest (94 cm) and highest (289 cm) measurements obtained from the experimental area (Table 5). Variation in depth occurs over relatively short distances (<100 m) and the range of values within individual blocks varies from 118 cm to 168 cm (Table 5). Interestingly there does not appear to be any correlation between the slope of the terrain (section 3.1.1) and peat depth, particularly given that Block A had the lowest slope (Table 3) and the lowest peat depth (Table 5).

4 Micro-relief components (nanotopes) and vegetation

4.1 Context

One of the consistent weaknesses in accounts of peat bog habitats, particularly in the UK, is the almost exclusive focus on vegetation assemblages without any reference to surface microtopography. This is unfortunate because the micro-relief of a bog surface – rather than vegetation – provides one of the most distinctive, characteristic and functionally informative components of a peat bog ecosystem (Lindsay, Riggall and Burd, 1985; Lindsay, 2010; Joosten *et al.*, 2017).

Peat bogs are often regarded as being relatively species poor compared with many other habitats. For the extensive tracts of *Eriophorum vaginatum* dominated blanket bog commonly seen across many parts of the uplands this may be so, but even these ‘dreary scenes’ (Rodwell, 1995) are species rich compared with the peat bogs of Tierra del Fuego where just one species of *Sphagnum* and two or three species of higher plants often comprise the dominant species assemblage for considerable expanses of peat bog landscape (Pisano, 1983). Despite their limited species composition, the bogs of Tierra del Fuego nevertheless display as much ecosystem diversity as the much-lauded peatlands of Scotland’s Flow Country (currently being considered for World Heritage Status) because small-scale structural features (nanotopes) created by the vegetation are arranged into repeating micro-relief patterns (microtopes), giving rise to complex self-regulating habitat-scale systems.

When external pressures, whether natural or anthropogenic, force change upon such systems, the resulting response occurs in both the vegetation and the microtopography. This response generally manifests itself in such a way that enables the self-regulating mechanisms of the system to compensate, thereby as far as possible maintaining system stability and continued peat accumulation (Barber, 1981; Ivanov, 1981; Couwenburg and Joosten, 2005). As Lindsay (2010) and Lindsay, Birnie and Clough (2014) highlight, increasing levels of degradation are associated with distinctive types of surface microtopography. Burning in particular tends to encourage dominance of fire-adapted species such as *Eriophorum vaginatum* and *Trichophorum cespitosum*. Loss of *Sphagnum* means that leaf bases in these vascular plant species no longer need to expend resources on elongating to out-compete *Sphagnum* growth. This results in a tight, dense tussock growth-form that resists fire and enables the plant to produce new shoots immediately after the fire has passed, thereby out-competing species that must recover from seed, plant fragments or underground parts (Weber, 1902; Wein, 1983; Lindsay 2010).

There is also evidence to indicate that burning affects the carbon density of at least the surface layers of a bog. With breakdown of the surface peat matrix as a result of burning, the smaller particles of peat will tend to pack together more tightly than in an open, loose carpet of living *Sphagnum*. This more tightly packed peat matrix also generally has a darker surface than a *Sphagnum* carpet and thus has a lower albedo, absorbing more solar radiant energy than a *Sphagnum* carpet which tends to turn papery white when dry, giving it an extremely high albedo. The denser peat matrix combined with increased warmth will tend to result in greater fluctuations in the water table which in turn leads to further decomposition of the peat matrix (Holden *et al.*, 2014; Holden *et al.*, 2015) see also:

<https://www.youtube.com/watch?v=DUFqrN1dxjU>

When fire has been severe or is a frequent event, tussock formation of the type described above is often accompanied by development of an interconnected network of micro-erosion occupying the ground between tussocks. Immediately following the fire, this micro-erosion network may consist almost entirely of ash and bare peat. Over time, however, and provided the tussocks are closely spaced, the shaded, damp environment provided by overhanging

leaves from the tussocks enables various moss species to become established and this, in turn, can eventually lead to colonisation by *Sphagnum* (Grosvernier, Matthey and Buttler., 1995; Sliva and Pfadenhauer, 1999). In the final phase of recovery, the *Sphagnum* overwhelms the tussock growth form, obliging the tussock-former to begin elongation of leaf-bases once again and thus develop a much looser growth in the form of individual leaves growing through the *Sphagnum* carpet (Weber, 1902; Lindsay, 2010).

The impact of grazing on microtopography is less well understood because the biological interactions between herbivores, plants and microtopography is rather poorly documented. Intense grazing is associated with development of bare peat as a result of weathering caused by trampling, and, at the very least, exacerbation of either pre-existing erosion, or by direct stimulation of erosion (Lindsay, Birnie and Clough, 2014; Chico *et al.*, 2019). Vegetation recovery of even badly damaged ground following reduction of grazing levels can occur within a decade or so, but there is little documented evidence for the response of the microtopography during the recovery process.

Within the context of the Hard Hill Experimental Plots, therefore, it might be expected that there would be some relationship between burning frequency, microtopography, peat density and vegetation, with grazing possibly adding another layer of impact.

4.2 Methods

Within the funding available it was not possible to undertake a full survey of all four blocks at Hard Hill. It was therefore decided that detailed investigation would be restricted to Block D but that the plots in the other three blocks would be recorded using VR technology to provide a set of baseline imagery for future reference.

4.2.1 VR imagery

A permanent metal marker, as described by Lindsay *et al.* (2019) for the IUCN 'Eyes on the Bog' programme, was inserted into the peat in the approximate centre of each plot in every block. The position was recorded using a Trimble R2 GNSS. A camera tripod was located over the metal marker and set to a height of 1.4 m. First a Theta Z1 360° 2D camera was placed on the tripod and a 360 panorama was obtained. Next an Insta360 camera set to 180° 3D format was placed on the tripod and a 180° stereo panorama was obtained for the view upslope. The camera was then turned through 180° to face downslope and a 180° 3D panorama obtained for that view.

For both sets of imagery – 360° and 180° – a large label was placed in the view with details of the plot management and the date marked clearly so that the image itself would contain the necessary details (see Figure 26).



Figure 26 Example of a 360° 2D view of the 1954-burn fenced treatment plot in Block D.

4.2.2 Peat density – use of penetrometer

It has been shown that blanket bog subject to burning tends to have a higher peat bulk density than areas of the habitat which have not been burnt, with attendant consequences for blanket bog hydrology (Holden *et al.*, 2014; Holden *et al.*, 2015). Given the pattern of regular burning across the Hard Hill plots, measurements of peat density were obtained in order to explore the pattern of bulk density associated with the differing treatment plots.

Furthermore, although it does not currently form part of any formal measure of habitat condition, the general ‘softness’ of a bog surface is often taken, albeit usually subconsciously, as an indication of peat bog habitat condition – the softer the general surface of the bog the better the condition-state. Potential development of a more formal way to assess peat bog condition using an index of ‘softness’ is currently being explored by the UEL Sustainability Research Institute (SRI). Data obtained for Hard Hill can therefore be compared with data obtained by UEL SRI from other sites.

Soil penetrometers are a standard means of testing the density of soils, but commercially available designs are unsuitable for use in most peat soils because peat is much less dense than most soils. Test readings tend to exceed the range of these penetrometers. Consequently, a penetrometer was constructed at UEL specifically for use on peat soils (see Figure 27). This consists of a threaded metal rod with a small top-plate. The rod is contained within an open Perspex cylinder which is placed vertically onto the peat. A weight is then dropped from a standard height onto the top-plate and the distance that the rod penetrates into the peat is noted.

Using the appropriate formula for low-speed projectile ballistics (http://panoptesv.com/RPGs/Equipment/Weapons/Projectile_physics.php) this gives a relative value of peat density based on ‘cavity strength’ (although the values cannot be used for geotechnical engineering purposes because several factors also then come into play – Dr Mike Long, UCD, *pers. comm.*).



Figure 27 Penetrometer for use on peat soils. (left) Components of the penetrometer. (right) Penetrometer in use in the field.

Cavity strength (y_c) was calculated thus:

$$Y_c = (mv^2)/2AX_p$$

where:

m = mass of dropped weight

v = velocity of weight on hitting the top-plate

A = cross-sectional area of threaded rod

X_p = penetration of threaded rod into the peat

Transects were laid out using a tape measure across each plot inside Block D at right angles to each fence post located along the long axis of the Block. With reference to the 1960s aerial photography, two additional plots were marked outside Block D: '1954 only' - in an area burnt in 1954 and 'Pre-1954' in an area not burnt in 1954 (see Figure 25). For each of the new plots transects were laid out on a spacing matching the mean distance between fence posts.

At 3 m intervals along each transect a penetrometer reading was obtained and the cavity strength of the peat at that point subsequently calculated. The start and end points of each transect were recorded using a Trimble R2 GNSS and the data post-processed using RINEX data from the OS Net base station located at Wearhead (13 km north-east). Positional data corrected to within 1.5 – 1.7 cm (x and y) and were used to determine accurate locations of each penetrometer reading in ArcGIS.

4.2.3 Bog microtopography and vegetation

At each of the locations along each transect where a penetrometer reading was obtained as described above, the nanotope type and vegetation type were also recorded. Both were noted according to the set of categories shown in Table 6.

Table 6 Categories used for nanotope and vegetation mapping – see also Section 24 of Lindsay (2010) for further details of nanotope types.

Nanotope category	Description
Tk - tussock	Dense tussock of either <i>Eriophorum vaginatum</i> or <i>Trichophorum cespitosum</i> .
ME – micro-erosion	Interconnected network of channels running between tussocks.
T3 – moss high hummock	The T3 high hummock zone of typical bog microtopography – formed by mosses rather than higher plants, the latter generally creating Tk tussocks. In the present case these T3 hummocks generally represent tussocks that have been overwhelmed by moss growth.
T2 – moss high ridge	The T2 high ridge zone of typical bog microtopography – formed by mosses rather than higher plants (the latter generally creating Tk tussocks). In the present case these areas of T2 high ridge generally represent areas of micro-erosion that have been overwhelmed by moss growth.
T1 – moss low ridge	The T1 low ridge zone of typical bog microtopography – formed by mosses and typically in this case representing early colonisation of micro-erosion gullies.
Vegetation category	
Sphagnum	Presence of Sphagnum – the species being noted.
Moss	Presence of mosses other than Sphagnum.
Dominant species forming the vegetation canopy were also noted.	For example, <i>Calluna vulgaris</i> , <i>Eriophorum angustifolium</i> , <i>Polytrichum commune</i> .

4.3 Results

4.3.1 VR imagery

The native imagery displayed very high contrast because the sky was much brighter than the ground, resulting in images in which the sky was washed out and the ground was too dark to see detail. The images were therefore processed using the RAW function in Adobe Photoshop to balance the brightness of the sky against the dark tone of the ground. Both the native imagery and the image-processed images have now been placed on the University of East London (UEL) Data Repository for permanent open-access storage. The imagery can be accessed using the following link: <https://repository.uel.ac.uk/item/87v0w> or the DOI: [doi:10.15123/uel.87v0w](https://doi.org/10.15123/uel.87v0w)

Instructions detailing how to download and view the imagery are provided as a ReadMe file within the metadata for the imagery in the links above.

It is anticipated that this image dataset will not merely illustrate the current state of each treatment plot but that it will form a long-term archive against which any future change can be assessed. The addition of 3D (stereo) to the image-set enables judgements to be made about the structure of the vegetation and the character of the nanotopes present.

Even when viewed using a smartphone and cheap VR viewer, the 3D imagery in particular highlights the differences in meso- and micro-relief displayed within the differing treatments, as already identified and discussed in Section(s) 3.1-3.2 of the present report. Images of the burnt-1954 plots in Block D, for example, reveal the linear 'erosion feature' running through the plots. Similarly, although the tussock density in the 10-year plots makes it difficult to see the micro-erosion network of bare peat beneath the vegetation cover, it is evident that many of the 10-year plots are relatively flat compared to the other treatments. The higher elevation and greater separation of the tussocks in many of the 20-year plots reveals the micro-eroded network more clearly, while many of the burnt-1954 plots show dominance of *Calluna vulgaris* on tussock/hummock tops but also senescence of leggy *Calluna*.

4.3.2 Penetrometer results – bulk density and bog 'softness'

Individual values for cavity strength along each transect line across the whole set of treatment plots can be seen in Figure 28. Each data point represents the value obtained from a single point along an individual transect, and the transects are grouped into treatment plots.

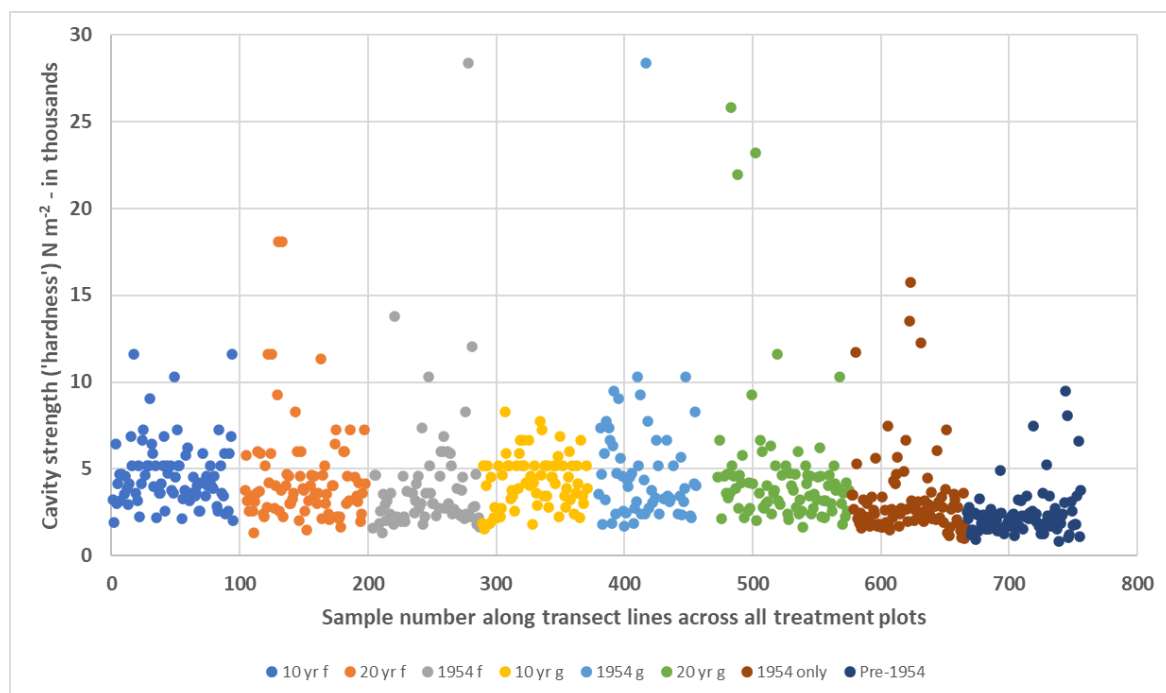


Figure 28 Individual values for cavity strength obtained from each sample point along each transect within Block D and in the new plots adjacent to Block D. Data points have been grouped into plot treatments. '10 yr f' = burnt every 10 years, fenced; '20 yr f' = burnt every 20 years, fenced; '1954 f' = burnt only in 1954, fenced; '10 yr g' = burnt every 10 years, grazed; '20 yr g' = burnt every 20 years, grazed; '1954 g' = burnt only in 1954, grazed; '1954 only' = new plot, burnt during the 1954 fire but located outside Block D, grazed; 'Pre-1954' = new plot, last burnt at some date prior to 1954 (potentially >95 years ago), grazed.

A broad overview of the data displayed in Figure 28 suggests a fairly consistent set of values between 1,000 and 5,000 N m⁻², then a wide scatter of points for values greater than 5,000 N m⁻². During field measurements it became evident that tussocks tended to give very high cavity strength values but were also highly variable. Heather roots and buried stems also gave high values but could be detected at the time of measurement because the penetrometer rod bounced markedly when hitting such material. If this occurred a replacement reading was taken slightly to the left or right of the initial point. The complete dataset therefore displays a high degree of variance almost entirely as a result of values obtained from tussocks. It might be argued, therefore, that in order to obtain a picture of condition for the bog surface as a whole, in general it is better not to sample tussocks because these will tend to generate consistently high values which may not reflect the overall condition of the plot.

Values greater than 9,000 N m⁻² were therefore excluded in order to remove the effect of the localised high values associated with the densest of the tussocks. Also excluded were those sample points clearly influenced by meso-scale features such as the deep 'trench' cutting through the 1954-burn treatment plots and the depressions/trackways made by persistent footfall from visiting researchers. The resulting distribution is shown in Figure 29. A general trend is evident, denser peat being broadly associated with the two 10-year plots and a more varied picture emerging from the 20-year plots and the 1954-burn plots. The most striking feature, however, is the relative frequency of low values (i.e. softer peat) within the two new supplementary plots, particularly in the Pre-1954-burn plot.

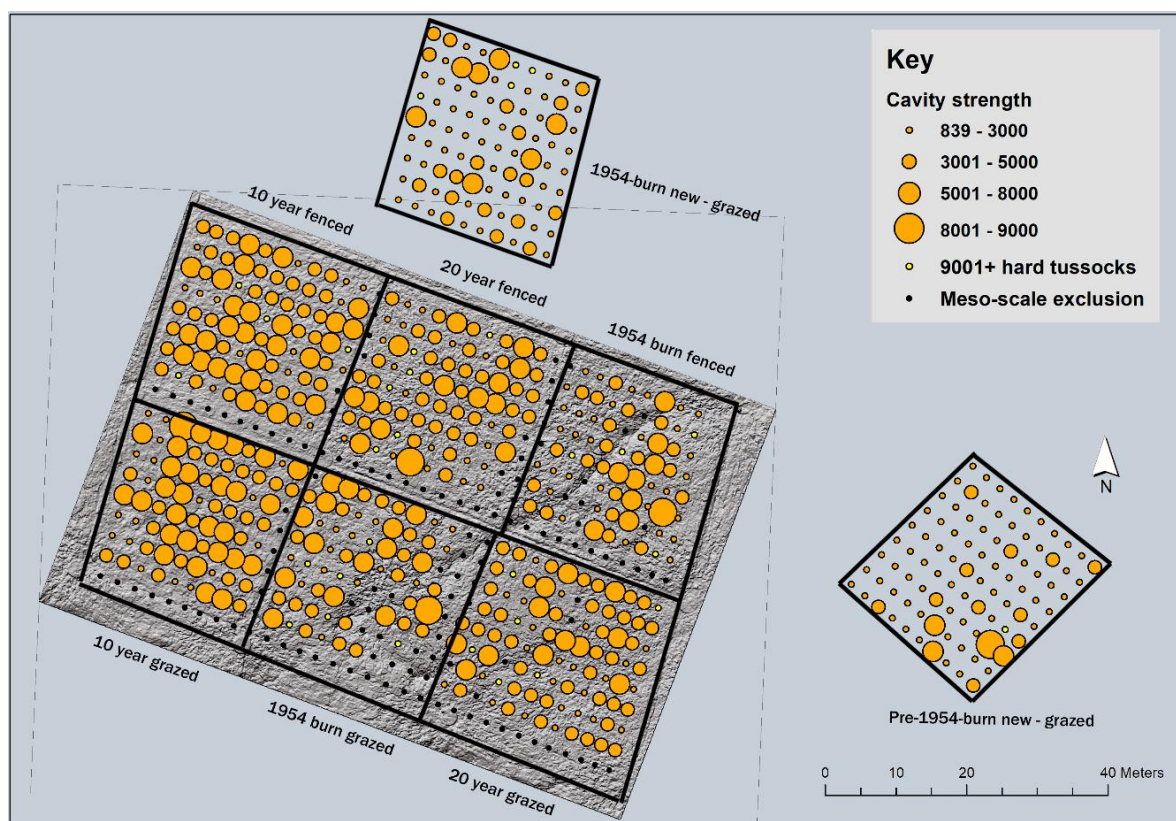


Figure 29 Map of cavity strength (i.e. peat 'hardness') for Block D and new supplementary plots, with sample points affected by meso-scale features removed (small black dots), and with the most dense tussocks indicated by pale yellow dots rather than cavity-strength values.

The data are also displayed as a box and whisker plot to highlight inter-quartile ranges, following which a more evident pattern begins to emerge (see Figure 30). While there is considerable overlap between the treatments, the fenced plots show a trend based on fire frequency, with the '1954 f' treatment possessing a greater quantity of softer ground than either the '10 yr f' treatment or the '20 yr f' treatment. Conversely the 10 yr f' treatment possesses a greater proportion of denser peat than any other treatment. Grazing appears to result in greater similarity between treatments, though the '20 yr g' treatment gives rise to somewhat softer values than the other two treatments. This plot lies at the foot of the slope on which Block D is located. The difference may thus be due to treatment but it may also be influenced by surface-water seepage and water accumulation within this treatment plot from the plots upslope.

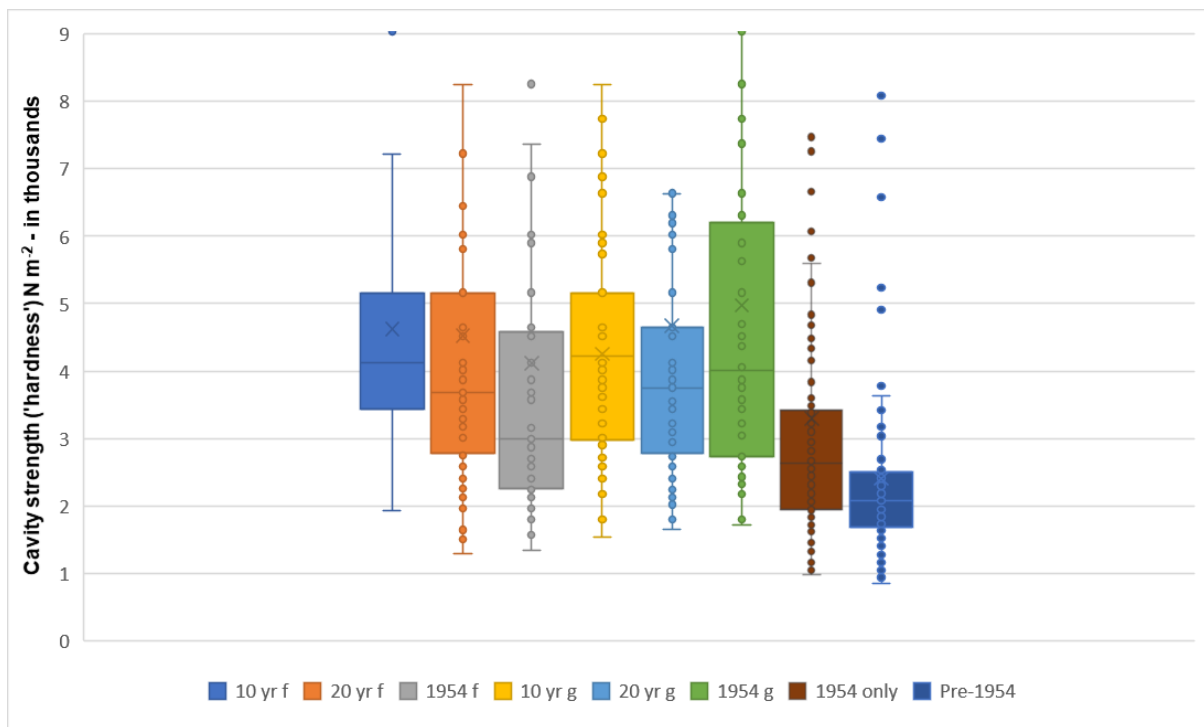


Figure 30 The data for cavity strength presented in Figure 28 now displayed as box plots, with the upper range of values truncated at 9,000 N m⁻² to remove the dense outliers largely representing tussocks. Data are grouped according to plot treatments. '10 yr f' = burnt every 10 years, fenced; '20 yr f' = burnt every 20 years, fenced; '1954 f' = burnt only in 1954, fenced; '10 yr g' = burnt every 10 years, grazed; '20 yr g' = burnt every 20 years, grazed; '1954 g' = burnt only in 1954, grazed; '1954 only' = new plot, burnt during the 1954 fire but located outside Block D, grazed; 'Pre-1954' = new plot, last burnt at some date prior to 1954 (potentially >95 years ago), grazed.

Although the new plot '1954 only' is located at the same elevation and same slope angle as the central part of Block D, being merely shifted to the north of Block D by some 20 m, the cavity strength values for this plot differ markedly from the plot subject to the same treatment within Block D. Indeed, the new '1954 only' plot displays cavity strength values that are generally lower (i.e. the ground is broadly softer) than values obtained for all treatments within Block D. Quite why this should be is not clear, although one possibility is that trampling pressure from repeated visits by researchers over the years has resulted in compression of the peat within Block D (and potentially also in the other three blocks). The new plot 'Pre-1954' that was not burnt in 1954 has evidently suffered fire damage at some time in the past because tussocks characteristic of such impact are still present. Nonetheless, this new plot gave rise to the lowest set of cavity strength values obtained during the survey – i.e. the ground was

generally softer than in any other treatment plot. Taking 'softness' as an indicator of bog condition, this might suggest that the Pre-1954' plot is in better condition than any of the other plots.

While there is a degree of correlation between peat density (as measured by cavity strength) and nanotope type, at least in the sense that tussocks tend to be associated with the highest values of cavity strength, measurements of peat density and 'softness' alone do not provide an adequate picture of the microtopography, nor of the vegetation types present. Both of these features do, however, provide information about the condition of a peat bog and thus complement data concerning softness of the bog surface.

Records for the microtopography and vegetation gathered alongside the cavity strength data display a variety of patterns that shed valuable light on the current state of the various treatment plots. The vegetation data can also be compared with vegetation data gathered during previous rounds of monitoring (alas, microtopography has not featured in these earlier rounds), thereby revealing trends over time at least for Block D.

4.3.3 Vegetation in Block D and additional plots

Lee et al. (2013) observe that 'peat-forming species' and particularly *Sphagnum* cover were recorded more frequently in the 10-year short-rotation burning plots during their survey in 2011, while Noble et al. (2018) analysed the historic data from 1961 and found no difference in *Sphagnum* cover between treatments at that earlier time but then found greater *Sphagnum* cover in the 10-year short-rotation burning plots in the most recent dataset. Balanced against this, both studies also found a more diverse *Sphagnum* assemblage in the Reference (R) plots – plots which may have been free from burning for more than 95 years. Both studies, however, based their comparisons on combined data for each treatment across all four blocks (A, B, C and D). Earlier parts of the present report highlight significant differences both within and between the four main blocks in terms of their meso-scale and micro-scale morphology. No such comparison has so far been made between the four original Reference plots. Differences between plots are particularly marked in Block D, where a major meso-scale feature, termed an 'erosion feature', runs through both of the '1954-burn' treatment plots.

It is therefore instructive to look at the earliest vegetation data available for Block D alone and compare it with the distribution of *Sphagnum* as recorded during the present survey of Block D. Figure 31 shows the cumulative Domin scores for all *Sphagnum* species recorded from Block D in 1961, thus presenting a picture of the relative cover of *Sphagnum* within each treatment plot. The relative cover of *Sphagnum* in the data from 1961 is markedly higher in both 10-year treatment plots and the fenced 20-year plot than in either of the 1954-burn plots. Moreover, quadrats of 1 m² recorded by Forrest (1961) list *Sphagnum* at Domin values of 8 or even 9, which means between 50% and 75% cover within the quadrat. It is most unlikely that *Sphagnum* could establish across a bare peat surface to this extent in only seven years, which suggests, firstly, that not all moss cover was removed by the fire in 1954, and secondly, that from the start of the experiment the plots burnt only in 1954 had a lower *Sphagnum* cover than the 10-year and 20-year treatment plots. Whilst the 1954-burn plots have now largely lost even those scattered *Sphagnum* individuals, the 10-year burn treatment plots have also experienced a substantial reduction in *Sphagnum* presence.

Several sample points in the 2019 survey corresponded closely with the quadrat locations of the 1961 survey yet no *Sphagnum* was recorded there in 2019. *Sphagnum* instead occurred as small scattered patches in 2019 rather than as major components of vegetation cover as the data indicate for 1961. If, as some have suggested, regular burning does indeed encourage *Sphagnum* growth then one might have expected after some 60 years of such

treatment to have seen extensive cover of *Sphagnum* that matched or exceeded the extent of cover recorded in 1961, rather than the scattered small-patch distribution currently observed.

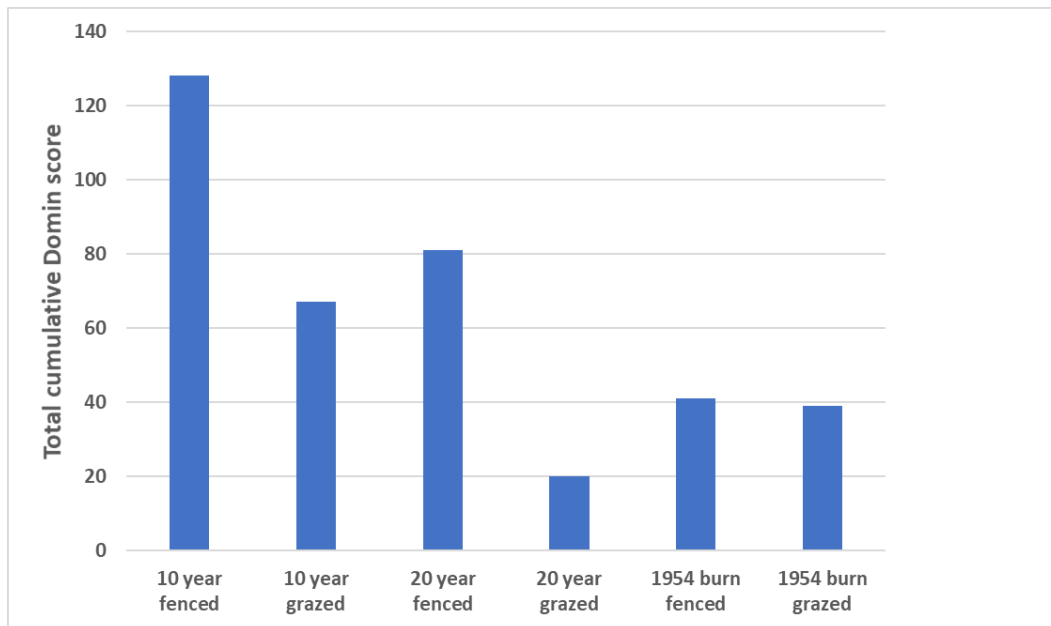


Figure 31 Total cumulative Domin scores for all *Sphagnum* species recorded in Block D in 1961 to show relative cover of *Sphagnum* in the six treatment plots of Block D.

Figure 32 also reveals that *Sphagnum* occurs in several localities within the newly-established plot positioned beyond the area burnt in 1954. Indeed, this new plot is the second-richest in *Sphagnum* across all the treatment plots of Block D despite not having been burnt for a period estimated, according to Rawes and Hobbs (1979) and the current duration of the experiment, to be in excess of 95 years (see Figure 33). Perhaps rather unexpectedly, the plot with the highest number of *Sphagnum* occurrences (though not necessarily % cover) is the 10-year grazed treatment. Such a pattern of occurrence has already been touched on above, but possible reasons for the greater number of occurrences compared with other treatments are also explored further in the Discussion of the present report.

It is also worth noting that the 20-year grazed plot has a concentration of *Sphagnum* records towards the southernmost corner of the plot. As explored earlier in the present report, this can perhaps be explained by the fact that the whole block slopes from NW to SE, so the southernmost corner of the 20-year grazed plot is the natural collecting point for water seeping across the block as a whole – or, given the presence of the meso-scale feature that cuts across the block, a collecting point for at least the lower third of the block.

This meso-scale erosion feature – possibly a sub-surface peat-pipe – creates what is in effect a drain line that cuts right through both 1954-burn treatment plots. It is perhaps not surprising, therefore, that what little *Sphagnum* cover existed in 1961 has now all-but disappeared, particularly given the vigorous growth of *Calluna vulgaris* encouraged by the drainage effects of this meso-scale feature. Beneath this aging *Calluna* canopy there is, however, a vigorous and extensive moss carpet consisting largely of *Hypnum jutlandicum*. Such a carpet can be an important early component of succession in which the moss cover overwhelms tussock nanotopes and provides a suitable environment for subsequent colonisation by *Sphagnum* species. The relationship between vegetation and nanotope is explored further in the next section.

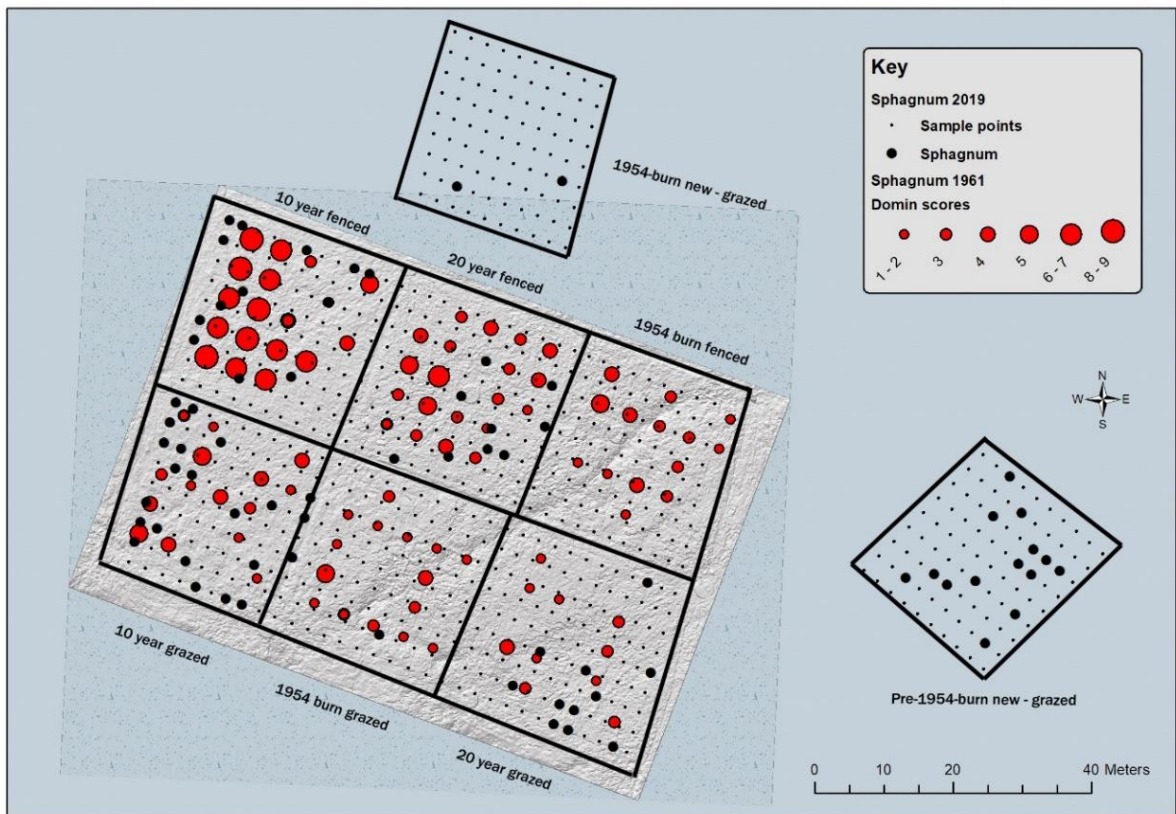


Figure 32 Distribution of *Sphagnum* cover in Block D for 1961 and 2019. Values for 1961 are Domin scores (sized red circles) while 2019 are presence/absence data (black circles). Small black dots indicate all sampling locations for 2019. The TLS ground survey data are displayed as background to the main Block D.

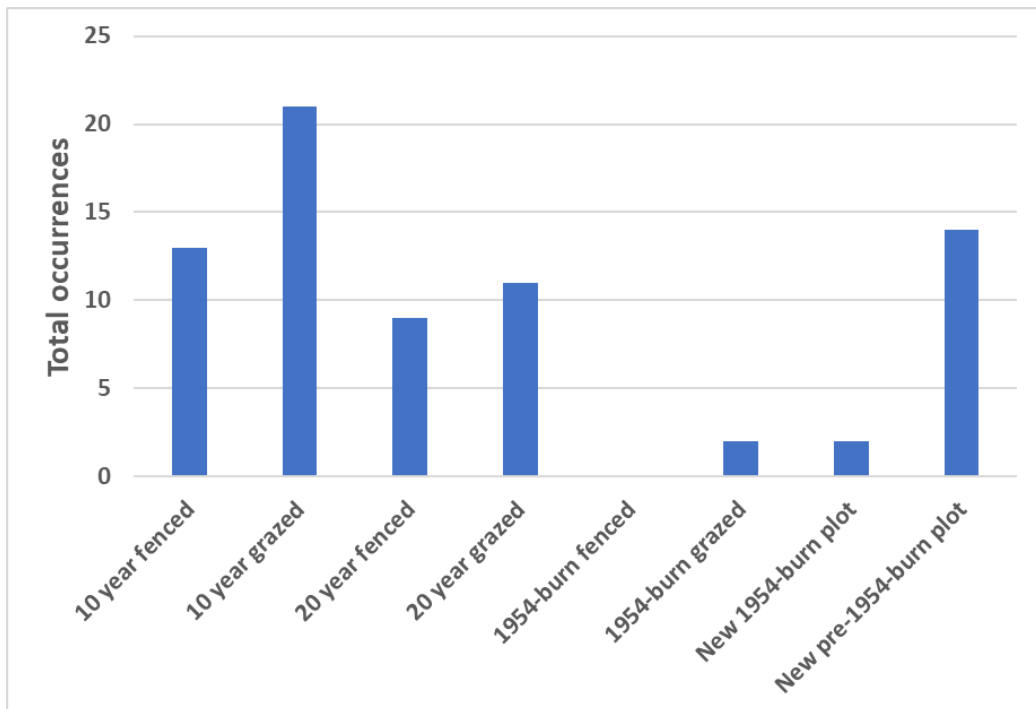


Figure 33 Cumulative occurrences of *Sphagnum* species within each treatment plot in Block D recorded in 2019.

In addition, during the course of the survey a decision was made to distinguish between mat-forming pleurocarpous mosses such as *Hypnum jutlandicum* and upright acrocarpous mosses such as *Funaria* and *Campylopus* species. Unfortunately, as this decision was made some way into the recording process it is not possible to present a consistent set of data for this, but the generally observed trend was for short acrocarpous mosses to be early colonisers of micro-erosion while mat-forming pleurocarpous mosses tended to be later colonisers, a pattern also observed by others (e.g. Harris et al., 2011; Lee et al., 2013). Further survey should incorporate this feature in order to provide a clearer picture of the contribution that differing moss life-forms make to the successional pattern.

In discussing the relative productivities of differing areas within Moor House, Forrest and Smith (1975) identify *Sphagnum* overgrowth of old *Calluna* as being a key factor in determining primary productivity and achieving a steady state in the vegetation:

“However, the adventitious rooting and rejuvenation of old Calluna stems caused by Sphagnum overgrowth almost certainly results in a higher total production than that of the two species growing independently. There is thus on the wetter blanket bog sites, in a steady state situation, an interesting example of the interaction of two species causing enhancement of total production.”

Just such a process of mutual support can be seen in some of the burnt-1954 only plots within the Hard Hill experiment, as well as in the newly established pre-1954 plot. Adventitious layering of *Calluna* within a *Sphagnum* hummock located in the Block D burnt-1954 grazed plot is shown in Figure 34.



Figure 34 Rejuvenated *Calluna* stems layering in a *Sphagnum capillifolium* hummock within the grazed, burnt-1954 only, Block D, treatment plot.

Looking more generally at the contrasting vegetation patterns found in particular between the treatment plots and the Reference plots, it is instructive to take the presence-absence data for both the treatment plots and the Reference plots presented by Lee et al. (2013) and sort the data using phytosociological methods. Such sorting is designed to draw out, without in any way altering the data, distinct species groupings that more often than not reveal ecologically meaningful assemblages (Müller-Dombois and Ellenberg, 1974).

The table of data presented by Lee et al. (2013) as part of their Supplemental data has thus been re-ordered using phytosociological principles and is shown in Appendix 1. Although some of the records (e.g. *Cladonia* spp.) are not helpful and some repetition may have arisen due to synonyms, the overall picture suggests that in the Reference plots there is evidence for development of a community characterised by a relatively species-rich *Sphagnum* assemblage and a low-growth canopy of *Calluna* together with fire-sensitive species such as *Neottia (Listera) cordata*.

Also striking is the dry heath-like community that in 1965 could be seen not only in the burnt-1954-only plots but also in the Reference plots, suggesting that the legacy of past burning, referred to by Forrest (1961) for the whole of Hard Hill and illustrated in the present report, could still be seen even in the Reference plots at that stage of the experiment, whereas by 2011 this legacy was much less pronounced within the Reference plots.

4.3.4 Nanotopes in Block D and additional plots

The basic sequence of peat bog recovery from fire is one of tussocks with micro-erosion nanotopes which are subsequently overgrown by moss-dominated communities in which either cotton grasses or *Calluna vulgaris* are the dominant vascular plants. *Sphagnum* is capable of colonising this damp moss community. *Sphagnum*, even being aided by the shade and humidity provided by the canopy of vascular plants (Forrest, 1961; Clymo and Hayward, 1982; Grosvernier et al., 1995; Sliva and Pfenner, 1999) finally re-establishes a microtopography based on the hummock-ridge-hollow structure of a natural bog surface.

This sequence is not the sole pattern observed, however. In some cases, *Sphagnum* can be found growing directly on bare peat within micro-erosion channels or growing within the mass of tussock-forming leaves, thereby short-circuiting succession and leading directly to a renewed *Sphagnum*-rich community. Examples of all these features, stages and processes can be seen in the Hard Hill plots.

It is therefore instructive to view the current pattern of nanotopes and vegetation observable within Block D in terms of tussocks and micro-erosion, moss communities and *Sphagnum*. It can be seen from Figure 35 that the dominant nanotope features of both the fenced and grazed 10-year plots and the fenced 20-year plot are micro-erosion and tussocks. Equally striking is the relative absence of micro-erosion from the 1954-burn treatment plots and the fact that the new pre-1954-burn plot recorded the lowest proportion of tussocks for any plot.

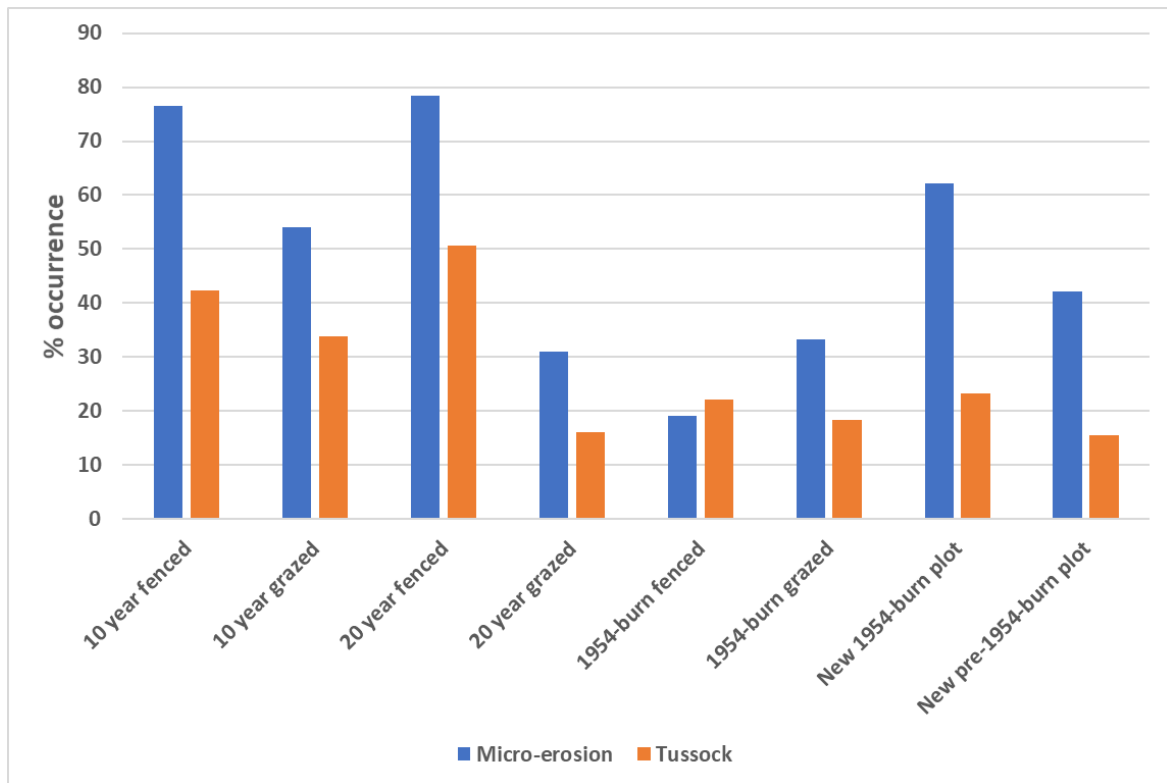


Figure 35 Percentage occurrence for micro-erosion and tussock nanotopes across the various plot treatments in Block D, based on sample points not affected by meso-scale features.

The relatively infrequent occurrence of both micro-erosion and tussocks in the 1954-burn plots may to some extent reflect the mid-stage of succession following fire, where a moss carpet begins to overwhelm both the tussocks and the micro-erosion network. It can also perhaps in part be explained by the presence of the meso-scale drainage feature running through both treatment plots. The microtopography appears to be somewhat suppressed by this feature, but it is also associated with vigorous growth of hypnoid mosses, mostly *Hypnum jutlandicum*, which results in an almost continuous bryophyte sward beneath the *Calluna vulgaris* associated with the line of the erosion feature (see Figure 36).

The contrast between the new 1954-burn plot with its 65-year recovery period and the newly established pre-1954-burn plot (estimated to be in excess of 95 years since the last fire) also points to a reduction in micro-erosion and tussocks, combined with an increase in *Sphagnum* occurrence. There is also a demonstrable association with the surface softness referred to in Section 4.3.2 of the present report, indicating recovery processes that extend beyond the 65-year post-fire interval represented by the new 1954-burn plot and the existing 1954-burn treatment plots.

It would be instructive to obtain micro-relief and softness measurements from the other three blocks at Hard Hill in order to determine whether this pattern is repeated across the whole study area. The VR imagery already obtained suggests that the pattern is indeed repeated, but now that a detailed set of information for slope has also been assembled, it may be that variations in the pattern of softness, micro-relief and vegetation will be influenced by this factor in addition to the effects of experimental treatment. The observations of Forrest and Smith (1975) and Rawes and Hobbs (1979) certainly suggest that this could be a likely outcome.

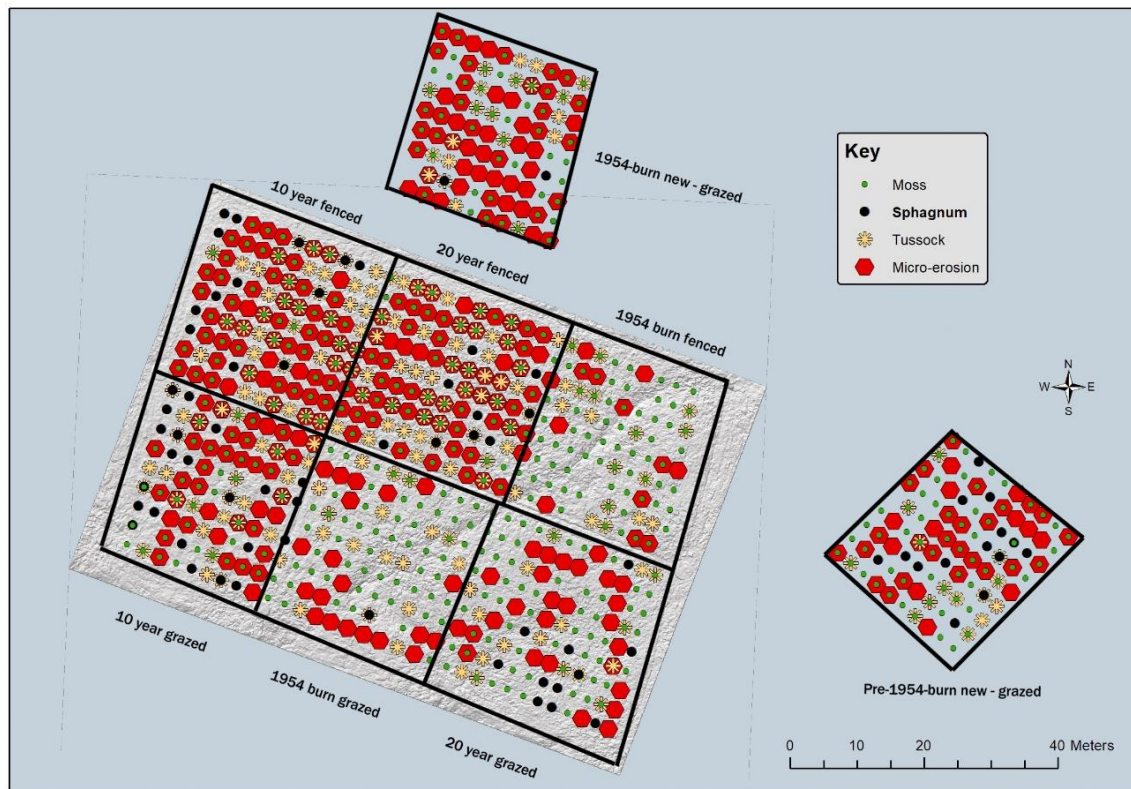


Figure 36 Distribution pattern of micro-erosion, tussocks, Sphagnum and hypnoid mosses across all plots associated with Block D. Different elements are displayed with the largest symbol to the rear and the smallest to the fore so that all co-occurrences can be seen. The meso-scale landscape features identified by TLS mapping within Block D are displayed as background for the six original treatment plots.

This pattern of micro-relief has considerable implications not merely for the immediate ecological character of the Hard Hill plots but also for a range of associated ecosystem services including some that influence the functioning of the wider landscape. While the function of peatlands acting as a ‘sponge’ within the landscape is now considered to be a far too simplistic view and indeed incorrect in many aspects, the role of natural micro-relief in adding ‘surface roughness’ to the landscape, slowing water movement and reducing flood peaks, remains an acknowledged benefit of such natural systems. This is partly because the natural micro-relief of a *Sphagnum*-rich surface tends to form undulations that lie across the line of water movement (Couwenberg and Joosten, 2005) but also because the semi-porous nature of the uppermost layer of a *Sphagnum* carpet – the acrotelm – acts as a responsive ‘valve’ influencing rates of water seepage downslope (Ivanov, 1981; Clymo, 1982; Ingram, 1982; Rydin and Jeglum, 2006).

Figures 37 & Figure 38 illustrate with actual examples the fundamentally differing character of a natural peat bog surface compared with one reduced by factors such as burning, grazing or atmospheric pollution to a tussock and micro-eroded surface. Figures 39 & 40 highlight the essential features of these two differing condition-states in diagrammatic form.



Figure 37 Differing examples of natural blanket bog systems. (left) *Sphagnum*/low dwarf shrub community; (centre) *Sphagnum*/cotton grass community; (right) *Sphagnum*/short sedge community. (left) Inverness-shire; (centre) Border Mires; (right) Sutherland.



Figure 38 Differing examples of degraded blanket bog systems dominated by tussock and micro-erosion from 10-year or 20-year treatment plots at Hard Hill. (left) *Calluna/Trichophorum*-bare peat; (centre) Cotton grass-bare peat; (right) Cotton grass/short mosses-bare peat.



Figure 39 A natural *Sphagnum*-rich bog surface has undulations that characteristically lie across the line of water movement. These undulations slow down seepage across the bog surface even if the peat is fully saturated.



Figure 40 A bog surface reduced to tussocks of cotton grass (*Eriophorum vaginatum*), deer-hair grass (*Trichophorum cespitosum*), purple-moor grass (*Molinia caerulea*) or wavy hair grass (*Deschampsia flexuosa*) with essentially bare peat between the tussocks has less capacity to slow down surface-water movement, even if there are occasional patches of *Sphagnum* or other mosses.

5 'Eyes on the Bog' long term markers

In addition to the permanent photo-location markers referred to in Section 4.3.1 of the present report, similar metal corner markers were also added to the two unmarked corners (i.e. the SE and SW corners) of Block D so that there are now fixed markers for these locations (see Figure 41).

Additional components of the IUCN UK Peatland Programme 'Eyes on the Bog' monitoring system were added to each treatment plot, in the form of surface-level markers and rust-rods. The former will provide an indication of carbon accumulation or loss from the plots as the ground surface changes over time, while the latter will indicate the long-term position of the water table relative to the surface. Two surface-level rods and five rust-rods were inserted within each plot and their location recorded using a Trimble R2 GNSS.



Figure 41 The visible blue top plate of a permanent metal marker indicates the SW corner of the grazed sector of Block D. Similar markers indicate the NW corner of the grazed sector as well as the fixed-photography points in the centres of each treatment plot.

Re-location of these markers once they become obscured by vegetation can be aided by the use of a simple metal detector, as illustrated in the 'Eyes on the Bog Manual' (Lindsay et al. 2019).

6 Synthesis

The Hard Hill Experiment is founded on the assumption that the four blocks and the treatment plots within these blocks provide replicates of the experimental treatments and thus provide statistical rigour to the experiment. Several anomalous aspects of the plots within the four blocks are identified by the present survey, raising questions about the appropriateness of treating the various plots as replicates of each other.

6.1 Meso-scale features within the treatment plots

The present survey has established evidence for substantial and ecologically significant meso-scale surface features within several of the Hard Hill treatment plots. It would seem that these meso-scale features have been present from the start of the experiment in 1954. In at least some instances these features have almost certainly had a more profound ecological effect on the vegetation and microtopography within the affected plots than the experimental interventions which the Hard Hill study sought to examine.

In Block D, for example, both 1954-burn treatment plots are substantially affected by what appears to be the sunken line of a sub-surface peat pipe that leads to the head of an adjacent stream course. The microtopography and vegetation of both plots appear to be closely tied to the effects of this feature, raising important questions about the validity of comparing these plots with the other plots in this Block and combining their data with other 1954-burn plots in other blocks. Meanwhile, in Block A, the fenced 1954-burn treatment plot is dominated by a shallow erosion complex that is revegetating. The hydrological implications of this feature also raise questions about the comparability of this plot with others in the block, irrespective of treatment effects.

6.2 Fire treatments within the individual plots

At the initiation of the experiment the vegetation on Hard Hill was assumed to be of comparable 'post fire' age, where all areas were reported to have been out of fire management for at least 30 (Rawes and Hobbs, 1979) or 40 (Hobbs, 1984) years. Six large burns were undertaken across the area in 1953/1954 and four of these burn scars were selected as areas in which to create the series of blocks and plots within which to replicate and monitor the impacts of future burning management. This study has revealed that when the experiment was initiated the vegetation across the area was not of comparable post-fire age. A large burn scar around 12-15 years old was present over half of the area that was established as Block B, and another burn scar estimated to be 15-30 years old was present in part of the area that became Block A. Differences in vegetation structure where these pre-experimental burn scars were present are visible in aerial photography captured in 1992, despite subsequent experimental fire management. This observation indicates not only the long-term impacts of burning on blanket bog vegetation, but that the vegetation within the plots affected are not comparable to other plots within the experiment.

It is also worth noting that the control of burning changed during the course of the experiment and inconsistent burn extents have resulted in a combination of vegetation age and repeat-interval within individual treatment plots. Comparison of vegetation across plots must exclude the areas having different burn ages at the start of the experiment as well as areas that have been burned inconsistently over time. To date, such exclusion has not formed a part of any published analyses.

6.3 Ecological condition of Block D and supplementary plots

Taking the broad pattern of burn frequency to range from the most frequent fires in the 10-year treatment plots compared with, at the other end of the scale, the new pre-1954-burn supplementary plot representing ground that has been without fire impacts for the longest period, it is possible to discern a composite ecological response to this fire-frequency gradient. Mirroring effects also found by previous authors, shorter fire-frequency intervals tend to be associated with denser peat whereas the plot with the longest fire-interval has the softest peat. There is also a tendency, albeit more variable, towards a microtopography dominated by micro-erosion and tussocks with shorter fire intervals whereas in the new plot that was not burnt in 1954, tussocks and micro-erosion are less frequent.

Micro-erosion offers a highly inter-connected drainage network encouraging comparatively rapid surface-water loss as well as a ready source of POC and DOC loss following rain events. As the micro-erosion complex becomes increasingly colonised by moss species this adds surface roughness to the micro-erosion channels and slows water movement. If the moss cover consists only of very low-growing acrocarpous mosses such as *Pohlia nutans* the effect on surface roughness is limited, but if the moss assemblage develops into thick mat-forming pleurocarpous mosses such as *Hypnum jutlandicum* the surface roughness of the channels increases substantially. If the channels become colonised by *Sphagnum* this has the potential to add considerably to surface roughness over time as well as also, over time, choking up and blocking the micro-erosion network to an extent that the rather looser mats of *Hypnum jutlandicum* are not able to achieve.

The 10-year and 20-year plots in Block D today possess more frequent *Sphagnum* than the 1954-burn plots, although the 10-year and 20-year fenced plots apparently possessed more *Sphagnum* than the 1954-burn plots at the start of the experiment. Today their *Sphagnum* cover seems to be significantly lower than at the start of the experiment. The new plot that was not burnt in 1954 has the second-highest frequency of *Sphagnum*, suggesting that whatever time-interval has elapsed since it was last burnt (an interval which is at present unknown but probably exceeds 95 years) is now sufficient for *Sphagnum* to be re-establishing a significant presence within the bog vegetation. It also brings into question the suggestion made by some authorities that not burning will ultimately lead to dense *Calluna* cover, drying out of the bog vegetation and loss of peat-forming species such as *Sphagnum*.

It is difficult to draw any clear conclusions about the presence in Block D of *Sphagnum* in the 10-year and 20-year plots relative to *Sphagnum* cover in the 1954-burn plots because the presence of the meso-scale trench cutting through both 1954-burn treatment plots confounds any possibility of identifying any effect of the experimental treatments alone. Conditions along the trench, particularly if it represents the line of a sub-surface peat pipe that may be directly draining the peat above it, are probably not conducive to *Sphagnum* growth or recovery, as is the altered surface morphology extending for some distance either side of the trench.

The new 1954-burn plot outside the main Block D has no such meso-scale feature and thus might be viewed as a more meaningful example of the 1954-burn treatment, although there are no 1961 data with which to compare the present very low *Sphagnum* cover. The continued high frequency of micro-erosion and tussocks in this plot suggests that the 1954 fire was possibly quite severe, but even if this is so there is still a greater presence of *Sphagnum* in the 10-year and 20-year treatment plots than in this new plot. While it is possible that this patch of blanket bog originally had less *Sphagnum* than the areas since managed on a 10-year or 20-year burning rotation, there are other factors worth considering.

Clymo (1983) highlighted the fact that fire passing over a peat surface can result in the condensation of water-repellent bitumens at the surface, while Hobbs (1986) states that burning of the peat surface can result in creation of a rubbery, gelatinous layer. Both effects

can give rise to small pockets of water retention at the surface into which *Sphagnum* fragments can colonise. This is, to some degree, a possible feedback system by which a bog surface may recover from burning and re-establish a peat-forming vegetation more rapidly than might otherwise be the case, but even this process requires time following the fire event for a *Sphagnum* carpet to develop.

The present position within both the 10-year and 20-year plots is that there are several small pockets of *Sphagnum* but there are no extensive swards of the kind suggested by the Domin values obtained for *Sphagnum* during the 1961 survey. In other words, although *Sphagnum* might be capable of colonising the regularly-burnt surfaces within the 10-year and 20-year treatment plots after the fire rotations, this repeated burning has prevented it from expanding significantly from these scattered locations and has resulted in an overall diminished cover compared with the position some 50 years ago. Had regular burning favoured *Sphagnum* growth it might be expected that the extent of *Sphagnum* observed in 1961 would have been further enhanced from its 1961 status, rather than diminished to the extent observed today.

The current relative absence of *Sphagnum* from the new 1954-burn plot may, as already observed, reflect the absence of *Sphagnum* on that ground when the experiment began in 1954, but it may also reflect a different, slower, pathway to recovery from that involving water-retaining pockets described immediately above but already outlined earlier in the present report. The role of tussocks and low moss carpets acting as 'nurse' environments for the eventual colonisation of damaged bog surfaces is a well-established sequence (Grosvernier *et al.*, 1995; Sliva and Pfadenhauer, 1999). This, however, takes time although in the end it offers the potential to re-develop a complete *Sphagnum*-rich peat-forming sward. The condition of the new pre-1954-burn plot and its *Sphagnum* cover suggests that time-to-recovery may be in the order of 95+ years. A similar picture emerges from the analysis undertaken by Lee *et al.* (2013) in which the original unburnt 'Reference Plots', thought to have been unburnt for at least 87 years, were found in 2011 to contain five species of *Sphagnum* not found in the treatment plots, as well as *Neottia (Listera) cordata* (Figure 42), which used to be common across the Pennine blanket bogs but had declined almost to local extinction by the inter-war years of the last century. It is a species characteristic of healthy *Sphagnum* swards beneath an open *Calluna vulgaris* canopy, being so strongly associated with moss carpets that it has been termed a 'bryophile' (Kotlínek, Tatarenko and Jersáková, 2018). Indeed, during the present survey one specimen was found some 20 m to the south of Block D within a *Sphagnum*-rich sward beneath an open *Calluna* canopy, though none was seen during the detailed survey of Block D.

Such long recovery times are commensurate with the natural pattern of fire frequencies on temperate and boreal peatland sites, where fire intervals are typically in the order of 150 years to 500 years yet subsequent recovery during the long intervals between fires has meant that overall peat accumulation has continued across millennial timescales (Hölzer and Hölzer, 1995; Sillasoo *et al.*, 2007; Rius, Vannièrè and Galop, 2009; van Bellen *et al.*, 2012). Thus, while the regularly-burnt plots within Block D may currently possess pockets of *Sphagnum*, the extent of these pockets is less than the cover noted in 1961, while the abundance of micro-erosion and tussocks after 65 years of experimental treatment suggests a system which is held in a form of arrested development. In contrast, the plots which have remained unburnt for the longest period, namely the new pre-1954-burn plot and the Reference Plots examined by Lee *et al.* (2013), are showing clear signs of re-developing a more typical natural bog community.

Interestingly, the one factor that appears to reflect duration-since-burning most closely is the density of the peat, as measured by the peat penetrometer. It would be instructive to carry out a full penetrometer survey of the remaining blocks to see whether this relationship is reflected consistently across the whole experiment.



Figure 42. Lesser twayblade (*Neottia [Listera] cordata*), a delicate 'sphagnophile' now recorded from the Reference plots but not yet recorded within the experimental plots.

7 Recommendations

Several recommendations can be made concerning issues arising from the present study:

- A survey of peat 'softness', nanotopes and vegetation types should be undertaken for Blocks A, B and C in order to obtain a complete picture of these key factors across the entire experimental array.
- Permanent fixed metal markers of the type used on Block D should be installed to indicate the corners of the grazed treatment plots on all four blocks in order to provide definitive reference points for the grazed plots.
- Surface-level rods and rust rods (as described for the IUCN 'Eyes on the Bog' programme) should be installed in each treatment plot of every block in order to provide long-term evidence for carbon accumulation or loss as well as for long-term water-table behaviour.
- Given the identified evidence for mis-application of burning treatments on some occasions in the past, plus the presence of existing burning scars within the experimental blocks, a re-examination of existing published data from the Hard Hill experiment taking these factors into account would appear to be a valuable exercise.
- Furthermore, given the identified evidence for substantial meso-scale structural features within some of the experimental blocks, any re-examination of existing published data from the Hard Hill experiment should also take these factors into account.
- Further plots should be established in the vicinity of the existing experimental blocks to replace those which have been shown to contain significant meso-scale features, and the fire history of these new plots should be established using historic aerial photography.

8 References

- BARBER, K.E. (1981) *Peat Stratigraphy and Climate Change: A palaeoecological test of the theory of cyclic peat bog vegetation*. Rotterdam: A.A.Balkema.
- BELL, J. (1843) New locality for *Saxifraga hirculus*. *The Phytologist*, 1, 741.
- CHICO, G., CLUTTERBUCK, B., MIDGLEY, N.G. and LABADZ, J. (2019) Application of terrestrial laser scanning to quantify surface changes in restored and degraded blanket bogs. *Mires and Peat*, 24(14), 1–24.
- CLUTTERBUCK, B (2015) *The surface micromorphology (microtopography) of the Hard Hill Burn Plots on Moor House – Upper Teesdale National Nature Reserve*. Final Report to Natural England. Peterborough.
- CLYMO, R.A. (1983) Peat. *In*: A.J.P. Gore (ed.) *Mires, Swamp, Fen and Moor. General Studies. Ecosystems of the World 4a*. pp.159-224. Amsterdam: Elsevier Scientific.
- CLYMO, R.A. (1983) Peat. *In*: A.J.P. Gore (ed.) *Mires, Swamp, Fen and Moor. General Studies. Ecosystems of the World 4a*. pp.159-224. Amsterdam: Elsevier Scientific.
- CLYMO, R. and HAYWARD, P.M. (1982) The Ecology of *Sphagnum*. *In*: A.J.E. Smith (ed.) *Bryophyte Ecology*. London: Chapman and Hall.
- COUWNEBERG, J. and JOOSTEN, H. (2005) Self-organization in raised bog patterning: the origin of microtope zonation and mesotope diversity. *Journal of Ecology*, **93** (6), 1238-1248.
- ELLIOTT, R.J. (1958). Experiments on burning. *In*: *The Nature Conservancy. A report of scientific work at the Moor House National Nature Reserve, Westmorland*.
- FORREST, G.I. (1961) *The effects of burning and grazing on a North Pennine moorland: August – September 1961*. Unpublished University College London report to the Nature Conservancy, Moor House National Nature Reserve.
- GROSVERNEIR, Ph., MATTHEY, Y. and BUTTLER, A. (1995) Microclimate and Physical Properties of Peat: New Clues to the Understanding of Bog Restoration Processes. *In*: B.D. Wheeler, S.C. Shaw, W.J. Fojt and R.A. Robertson (eds.) *Restoration of Temperate Wetlands*. pp. 435-450. Chichester: John Wiley & Sons.
- HARRIS, M.P.K., ALLEN, K.A., McALLISTER, H.A., EYRE, G., LE DUC, M.G. and MARRS, R.H. (2011) Factors affecting moorland plant communities and component species in relation to prescribed burning. *Journal of Applied Ecology*, **48**, 1411-1421
- HOBBS, R.J. (1984) Length of burning rotation and community composition in high-level *Calluna-Eriophorum* bog in N England. *Vegetatio*, 57, 129-136.
- HOBBS, N.B. (1986) Mire morphology and the properties and behaviour of some British and foreign peats. *Quarterly Journal of Engineering Geology*, **19**, 7-80.
- HOLDEN, J., PALMER, S.M., JOHNSTON, K., WEARING, C., IRVINE, B. and BROWN, L.E. (2015) Impact of prescribed burning on blanket peat hydrology. *Water Resources Research*, **51**(8), 6472–6484.

HOLDEN, J., WEARING, C., PALMER, S.M., JACKSON, B., JOHNSTON, K. and BROWN, L.E. (2014) Fire decreases near-surface hydraulic conductivity and macropore flow in blanket peat. *Hydrological Processes*, **28**, 2868–2876. doi:10.1002/hyp.9875

HÖLZER, A. and HÖLZER, A. (1995) *Zur Vegetationsgeschichte des Hornisgrinde-Gebietes im Nordschwarzwald: Pollen, Grossteste und Geochemie* [On the history of vegetation in the Hornisgrinde area in the northern Black Forest: pollen, macrofossils and geochemistry]. *Carolinea*, **53**, 199-228.

INGRAM, H.A.P. (1983) Hydrology. In: A.J.P. Gore (ed.) *Mires, Swamp, Fen and Moor. General Studies. Ecosystems of the World 4a*. pp.67-158. Amsterdam: Elsevier Scientific.

IVANOV, K.E. (1981) *Water Movement in Mirelands*. [English translation by A. Thompson and H.A.P. Ingram]. London: Academic Press.

JOOSTEN, H., MOEN, A., COUWENBERG, J. and TANNEBERGER, F. (2017) Mire diversity in Europe: mire and peatland types. In: H. Joosten, F. Tanneberger and A. Moen (eds.) *Mires and Peatlands of Europe: Status, distribution and conservation*. pp. 5-64. Stuttgart: Schweitzerbart Science Publishers.

KOTILÍNEK, M., TATARENKO, M. and JERSÁKOVÁ, J. (2018) Biological Flora of the British Isles: *Neottia cordata*. *Journal of Ecology*, **106**, 444–460.

LEE, H., ALDAY, J.G., ROSE, R.J., O'REILLY, J. and MARRS, R.H. (2013) Long-term effects of rotational prescribed burning and low-intensity sheep grazing on blanket-bog plant communities. *Journal of Applied Ecology*, 50(3), 625–35. doi.org/10.1111/1365-2664.12078

LINDSAY, R.A. (2010) *Peatbogs and carbon: a critical synthesis to inform policy development in oceanic peat bog conservation and restoration in the context of climate change*. Commissioned Report to the Royal Society for the Protection of Birds (RSPB). Available from: <https://repository.uel.ac.uk/item/862y6>

LINDSAY, R., BIRNIE, R. and CLOUGH, J. (2014) *Peat Bog Ecosystems: Structure, Form, State and Condition*. Edinburgh International Union for the Conservation of Nature. Available from: <https://repository.uel.ac.uk/item/85872>

LINDSAY, R.A., RIGGALL, J. and BURD, F. (1985) The use of small-scale surface patterns in the classification of British peatlands. *Aquilo, Seria Botanica*, **21**, 69-79. Available from: <https://repository.uel.ac.uk/item/86qv8>

MÜLLER-DOMBOIS, D. and ELLENBERG, H. (1974) *Aims and methods of vegetation ecology*. New York: John Wiley and Sons.

NOBLE, A., O'REILLY, J., GLAVES, D.J., CROWLE, A., PALMER, S.M. and HOLDEN, J. (2018) Impacts of prescribed burning on *Sphagnum* mosses in a long-term peatland field experiment. *PLoS ONE*, **13**(11): e0206320. <https://doi.org/10.1371/journal.pone.0206320>

PISANO, E. (1983) The Magellanic Tundra Complex. In: A.J.P. Gore (ed.) *Mires: Swamp, Bog, Fen and Moor. (Ecosystems of the World 4B) Regional Studies.*, 295--329. Amsterdam, Elsevier Scientific.

RAWES, M. (1964) *Report on burning programme*. Unpublished Nature Conservancy report, Moor House National Nature Reserve.

RAWES, M. (1965) *1965 report*. Unpublished Nature Conservancy report, Moor House National Nature Reserve.

RAWES, M. and HOBBS, R. (1979) Management of Semi-Natural Blanket Bog in the Northern Pennines. *Journal of Ecology*, 67(3), 789-807.

RIUS, D., VANNIÈRE, B. and GALOP, D. (2009) Fire frequency and landscape management in the northwestern Pyrenean piedmont, France, since the early Neolithic (8000 cal. BP). *The Holocene*, 19 (6), 847-859.

RODWELL, J.S. (1991) *British Plant Communities: Vol. 2, Mires and Heaths*. Cambridge: Cambridge University Press.

RYDIN, H. and JEGLUM, J.K. (2006) *The Biology of Peatlands*. Oxford: Oxford University Press.

SILLASOO, Ü., MAUQUOY, D., BLUNDELL, A., CHARMAN, D., BLAAUW, M., DANIELL, J.R.G., TOMS, P., NEWERRY, J., CHAMBERS, F.M. and KAROFELD, E. (2007) Peat multi-proxy data from Männikjärve bog as indicators of late Holocene climate changes in Estonia. *Boreas*, 36, 20-37.

SLIVA, J. and PFADENHAUER, J. (1999) Restoration of cut-over raised bogs in southern Germany – a comparison of methods. *Applied Vegetation Science*, 2, 137-148.

TAYLOR, P. and RAWES, M. (1974) Aspects of the ecology of the northern Pennines. The ecology of the Red Grouse. Occasional Papers No.6.

van BELLEN, S., GARNEAU, M., ALI, A.A. and BERGERON, Y. (2012) Did fires drive Holocene carbon sequestration in boreal ombrotrophic peatlands of eastern Canada? *Quaternary Research*, 78, 50–59.

WEBER, C.A. (1902) *Über die Vegetation und Entstehung des Hochmoors von Augstumal im Memeldelta* [Vegetation and Development of the Raised Bog of Augstumal in the Memel delta.]. Berlin: Verlagsbuchhandlung Paul Parey. : English transl. In: J. Couwenberg and H. Joosten (eds.) (2002) *C.A. Weber and the Raised Bog of Augstumal*. Tula, Russia: International Mire Conservation Group/PPE “Grif & K”].

WEIN, R.W. (1983) Fire behaviour and ecological effects in organic terrain. In: R.W. Wein and D.A. MacLean (eds.) *The Role of Fire in Northern Circumpolar Ecosystems*. pp. 81-95. Chichester: Wiley.

Websites

The physics of projectile ballistics website

http://panoptesv.com/RPGs/Equipment/Weapons/Projectile_physics.php

Accessed: 20th February 2020

Appendix 1

Re-working of data from Lee et al. (2013)

Table 7 presents an analysis using phytosociological sorting, as set out in Müller-Dombois and Ellenberg (1974), of presence-absence species data assembled by Lee et al. (2013 Supplementary Table S2) for the Hard Hill Experimental Plots, comparing in particular the species data for the treatment plots against species data for the Reference plots that were estimated to have been unburnt for at least 87 years.

The data presented by Lee et al. (2013) remain unaltered but have been re-ordered according to phytosociological principles to highlight ecological groupings of species. Some of the species/attribute listings from Lee et al. (2013) are of doubtful value or quality, but all have been included here so as not to alter the data in any way. Data for 1965 consist only of records for the 'burnt 1954 only' plots (N) and the Reference plots (R). Data for 1961, 1973, 1982, 1992 and 2001 represent the combined results obtained from the experimental plots (burnt 1954 only, short 10-year rotation, long 20-year rotation – N/S/L), while in 2011 the Reference plots (or at least areas very close to these plots) were again surveyed.

Table 7 Presence-absence species data assembled by Lee et al. (2013) presented using phytosociological sorting.

Year of survey	'11	'01	'73	'82	'92	'61	'65	'65
Burning treatment	R	N/S/L	N/S/L	N/S/L	N/S/L	N/S/L	N	R
Damp Sphagnum/moss-rich (beneath dwarf shrub)								
<i>Hylocomium splendens</i>	√							
<i>Hypnum imponens</i>	√							
<i>Mnium hornum</i>	√							
<i>Sphagnum capillifolium</i> <i>subsp. capillifolium</i>	√							
<i>Sphagnum fimbriatum</i>	√							
<i>Sphagnum magellanicum</i>	√							
<i>Sphagnum subnitens</i>	√							
<i>Sphagnum tenellum</i>	√							
<i>Cephaloziella sp.</i>	√							
<i>Neottia (Listera) cordata</i>	√							
Slightly damaged/enriched Sphagnum/moss community								
<i>Campylopus introflexus</i>	√	√						
<i>Kindbergia praelonga</i>	√	√						
<i>Sphagnum russowii</i>	√	√						
<i>Calypogeia muelleriana</i>	√	√						
<i>Dryopteris dilatata</i>		√						
<i>Sphagnum molle</i>		√						
<i>Cephaloziella divaricata</i>		√						
<i>Cladonia diversa</i>		√						

<i>Sphagnum fallax</i>	√	√				√		
Damp bare peat with moss and liverworts								
<i>Lepidozia reptans</i>	√		√					
<i>Rhytidiadelphus loreus</i>	√	√	√					
<i>Polytrichum strictum</i>	√		√	√				
Litter	√	√	√	√	√			
<i>Lophocolea bidentata</i>	√	√	√	√	√			
<i>Calypogeia fissa</i>	√				√			
<i>Polytrichum sp.</i>		√						
<i>Sphagnum capillifolium</i>		√	√	√	√			
<i>Diplophyllum albicans</i>		√	√	√	√			
<i>Cladonia furcata</i>			√	√	√			
<i>Cladonia sp.</i>			√	√				
<i>Sphagnum palustre</i>			√					
Open water				√				
<i>Cladonia fimbriata</i>				√				
<i>Plagiomnium undulatum</i>		√				√		
Dry/damaged bog								
<i>Plagiothecium laetum</i>					√			
<i>Trichophorum cespitosum</i>		√	√	√	√	√		
<i>Polytrichum commune</i>		√	√	√	√	√		
<i>Cladonia chlorophaea</i>			√	√	√	√		
<i>Sphagnum cuspidatum</i>	√					√		
<i>Sphagnum papillosum</i>			√			√		
<i>Odontoschisma sphagni</i>		√				√		
<i>Cladonia uncialis</i>			√			√		
<i>Tetraphis pellucida</i>			√	√	√		√	
Dry heath								
<i>Cladonia scabriuscula</i>						√		
<i>Deschampsia cespitosa</i>						√		
<i>Racomitrium lanuginosum</i>						√		
<i>Splachnum sphaericum</i>						√		
<i>Cladonia cariosa</i>						√		
<i>Cladonia crispate</i>						√		
<i>Hypogymnia physodes</i>			√	√		√	√	√
<i>Cladonia floerkeana</i>						√	√	
<i>Polytrichum piliferum</i>						√	√	
<i>Cladonia ciliata</i>	√						√	√
<i>Sphagnum capillifolium subsp. rubellum</i>	√					√	√	√
<i>Cladonia arbuscula</i>						√	√	√
<i>Cladonia pyxidata</i>						√	√	√

<i>Trapeliopsis granulosa</i>						√	√	√
<i>Cladonia coccifera</i>						√	√	
Community constants								
<i>Calluna vulgaris</i>	√	√	√	√	√	√	√	√
<i>Empetrum nigrum nigrum</i>	√	√	√	√	√	√	√	√
<i>Eriophorum angustifolium</i>	√	√	√	√	√	√	√	√
<i>Eriophorum vaginatum</i>	√	√	√	√	√	√	√	√
<i>Rubus chamaemorus</i>	√	√	√	√	√	√	√	√
<i>Vaccinium myrtillus</i>	√	√	√	√	√	√	√	√
<i>Vaccinium vitis-idaea</i>	√	√	√	√	√	√	√	√
<i>Aulacomnium palustre</i>	√	√	√	√	√	√	√	√
<i>Campylopus flexuosus</i>	√	√	√	√	√	√	√	√
<i>Dicranum scoparium</i>	√	√	√	√	√	√	√	√
<i>Pohlia nutans</i>	√	√	√	√	√	√	√	√
<i>Rhytidiadelphus squarrosus</i>	√	√	√	√	√	√	√	√
<i>Cephalozia bicuspidata</i>	√	√	√	√	√	√	√	√
<i>Lophozia ventricosa</i>	√	√	√	√	√	√	√	√
Companion species								
<i>Bare soil</i>	√	√	√	√	√	√		
<i>Green Algae</i>	√	√	√	√	√	√		
<i>Pleurozium schreberi</i>	√	√	√	√	√	√		
<i>Cladonia portentosa</i>	√	√	√	√	√	√		
<i>Mylia taylorii</i>		√	√	√	√	√	√	√
<i>Calypogeia azurea</i>			√	√	√	√	√	√
<i>Mylia anomala</i>			√	√	√	√	√	√
<i>Cladonia squamosa</i>			√	√	√	√	√	√
<i>Cephalozia connivens</i>	√		√	√	√	√	√	√
<i>Ptilidium ciliare</i>	√	√	√	√	√	√		√
<i>Plagiothecium undulatum</i>	√		√	√		√	√	√
<i>Barbilophozia floerkei</i>	√		√	√	√	√		√
<i>Hypnum jutlandicum</i>	√	√	√	√	√	√	√	
<i>Kurzia pauciflora</i>	√	√	√	√	√	√	√	